Journal of Medicinal Chemistry

pubs.acs.org/jmc

Article

Development of Covalent, Clickable Probes for Adenosine A_1 and A_3 Receptors

Phuc N. H. Trinh, Daniel J. W. Chong, Katie Leach, Stephen J. Hill, Joel D. A. Tyndall, Lauren T. May,* Andrea J. Vernall,* and Karen J. Gregory*

Cite This: *J. Med. Chem.* 2021, 64, 8161−8178

Read Online

ACCESS | Metrics & More | Article Recommendations | Supporting Information

ABSTRACT: Adenosine receptors are attractive therapeutic targets for multiple conditions, including ischemia-reperfusion injury and neuropathic pain. Adenosine receptor drug discovery efforts would be facilitated by the development of appropriate tools to assist in target validation and direct receptor visualization in different native environments. We report the development of the first bifunctional (chemoreactive and clickable) ligands for the adenosine A_1 receptor (A_1R) and adenosine A_3 receptor (A_3R) based on an orthosteric antagonist xanthine-based scaffold and on an existing structure−activity relationship. Bifunctional ligands were functional antagonists with nanomolar affinity and irreversible binding at the A_1R and A_3R. In-depth pharmacological profiling of these bifunctional ligands showed moderate selectivity over A_{2A} and A_{2B} adenosine receptors. Once bound to the receptor, ligands were successfully "clicked" with a cyanine-5 fluorophore containing the complementary "click" partner, enabling receptor detection. These bifunctional ligands are expected to aid in the understanding of A_1R and A_3R localization and trafficking in native cells and living systems.

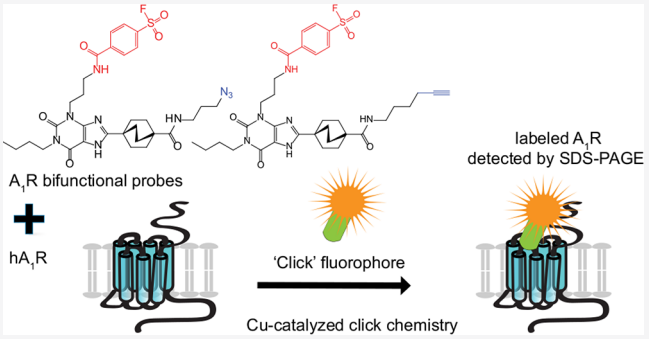

INTRODUCTION

The adenosine receptor (AR) family consists of four (A_1, A_{2A}, A_{2B}, and A_3) cell surface G protein-coupled receptor (GPCRs) subtypes that are activated by adenosine, an endogenous purine nucleoside present both intracellularly and extracellularly in living cells.[1−3] Among the AR subtypes, the A_1R remains a highly pursued therapeutic target for a number of neurological, cardiovascular, and renal pathologies. Activation of the A_1R minimizes cardiac and renal ischemia-reperfusion injury, atrial fibrillation, and neuropathic pain, whereas A_1R inhibition can enhance diuresis and cognition.[4−8] Despite significant efforts, selective A_1R agonists or antagonists have not transitioned into the clinic, typically due to a lack of on-target efficacy or adverse effects.[9] In addition, traditional discovery pipelines have taken a limited view of A_1R activity often relying on a single measure of receptor activation to guide hit progression. However, we and others have shown that biased agonism is operative at the A_1R, raising the possibility that not all aspects of A_1R drug action have been fully elucidated.[9−11] One of the major challenges faced in A_1R drug discovery is a need for specific tools for target engagement and to study noncanonical measures of receptor behavior that have gone unappreciated when assessing A_1R ligands in traditional pipelines, such as receptor internalization and localization.

Antibody-based approaches are commonly employed to localize proteins of interest in different tissues or subcellular compartments; however, GPCR-targeting antibodies notoriously lack specificity, and specific antibodies against the A_1R are lacking. Chemical probes such as "preassembled" A_1R fluorescent ligands have been developed to interrogate A_1R function.[12−14] However, large fluorescent ligands also come with challenges; for example, the fluorescent moieties may interfere with receptor affinity or selectivity.[15−17] Furthermore, the chemical synthesis and detailed characterization required for each preassembled fluorescent ligand limits the number of different fluorophores that can be incorporated. Breaking up a preassembled fluorescent ligand into two parts with a complementary "clickable" handle installed on each offers an alternative and advantageous "in situ labeling" solution to the conventional binding of a single high-molecular weight fluorescent ligand. This strategy creates a bifunctional ligand that requires a two-step labeling approach to detect GPCRs. The first step involves covalent attachment of either a chemoreactive or photoreactive ligand to the receptor, followed by incorporation of a reporter (e.g., a fluorophore or biotin) using a

Received: December 16, 2020
Published: June 14, 2021

https://doi.org/10.1021/acs.jmedchem.0c02169
J. Med. Chem. 2021, 64, 8161−8178

bioorthogonal reaction (e.g., click chemistry). The feasibility of this two-step labeling approach has been demonstrated for multiple GPCRs, including metabotropic glutamate receptor subtypes 2[18] and 5,[19] cannabinoid CB_2 receptors,[20] and adenosine A_{2A} receptors.[21] Importantly, relying on conjugation between two functional groups that are foreign to the biological system offers exquisite selectivity. For example, bifunctional cannabinoid CB_2 receptor ligands enabled profiling of endogenous receptor expression levels in peripheral blood mononuclear cells by fluorescence-activated cell sorting.[20] Combining bioorthogonal labeling with advanced imaging approaches has the potential to yield great insights into endogenous receptor localization and target engagement in different cell and tissue types. Our two-step approach also has significant advantages over a bespoke "preassembled" fluorescent ligand in that different fluorophores can be tethered, akin to the HaloTag and SNAP-tag technology, and fluorophores appropriate for a range of different fluorescent techniques, including time-resolved fluorescence resonance energy transfer (TR-FRET) experiments, could be incorporated.

Fluorescent ligand design is often facilitated by detailed structural information gained from X-ray crystallographic and cryo-electron microscopic protein structures. In recent years, the amount of structural information for GPCRs has increased rapidly and is immensely helpful to interrogate ligand−receptor interactions. The recently determined A_1R crystal structure (PDB entry 5UEN)[22] complexed with xanthine-based antagonist DU172 (**1**) (Figure 1) showed a covalent bond between the

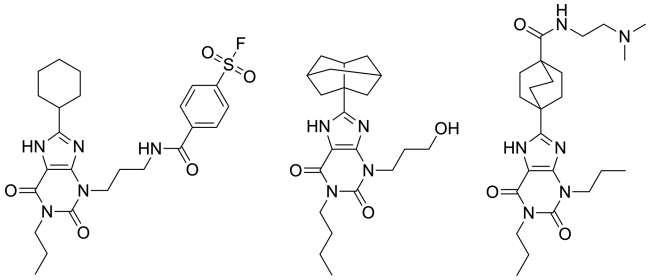

Figure 1. A_1R ligands DU172 (**1**), PSB36 (**2**), and **3**.

DU172 sulfonyl moiety and Y271$^{7.36}$ (Ballesteros−Weinstein numbering in superscript) and the cyclohexyl group positioned toward the top of the receptor surrounded by residues M177$^{5.35}$, L253$^{6.54}$, and T257$^{6.57}$. Subsequently, the co-crystal structure of A_1R with orthosteric antagonist PSB36 (**2**) (Figure 1) (PDB entry 5N2S)[23] showed PSB36 resides deeper in the A_1R binding pocket than in the $A_{2A}R$. In particular, the N1-butyl of PSB36 was directed toward a hydrophobic pocket of V87$^{3.32}$, L88$^{3.33}$, A91$^{3.36}$, M180$^{5.38}$, W247$^{6.48}$, and H251$^{6.52}$ in the A_1R while this region appeared to be less accessible in the $A_{2A}R$.[23] There have been many SAR studies of xanthine-based AR ligands. Notably, xanthine C8-bicyclo[2.2.2]octyl derivatives with varying extensions from the bicyclo ring improved A_1R selectivity [for example, **3** (Figure 1)].[24] Herein, we describe the rational design, synthesis, and evaluation of bifunctional (covalent and clickable) ligands for the A_1R.

RESULTS AND DISCUSSION

Ligand Design. The design of the bifunctional ligands was inspired by features of DU172 and A_1R antagonists such as **3** with a C8-bicyclo[2.2.2]octyl that conferred A_1R selectivity.[24] A xanthine N1-butyl (as opposed to propyl) alkyl chain was hypothesized to imbue A_1R selectivity because of the deeper hydrophobic pocket apparent in the A_1R (PDB entry 5UEN).[22] A bicyclo[2.2.2]octyl group was appended from the xanthine C8 with the aim of achieving excellent A_1R affinity and selectivity as has previously been reported. The bicyclo[2.2.2]octane-1,4-dicarboxylic acid moiety was also advantageous over using a cyclohexyl moiety with *cis,trans* isomer complications. Analogous to DU172, a sulfonyl fluoride warhead capable of potentially covalently binding to Y271$^{7.36}$ of the A_1R was installed. A similarly positioned tyrosine is also present in the $A_{2A}R$ (Y271) and A_3R (Y265$^{7.36}$), but the use of the bicyclo[2.2.2]octyl group, based on SAR, was hypothesized to provide A_1R selectivity. The bifunctional ligands also required a linker terminating in a "clickable" functional group. Linkers were appended in an analogous position to the ethyl dimethylamine of **3** for two reasons. (1) Variations in this part of the molecule can retain A_1R affinity,[24] and (2) on the basis of the position of DU172 in PDB entry 5UEN, it was envisaged that a linker installed from this part of the ligand would be exposed to the receptor surface and accessible for a "click" reaction. The "clickable" handle design consisted of either an azide or an alkyne, which could undergo a Huisgen 1,3-dipolar cycloaddition reaction with the complementary partner of, for example, a fluorophore, forming a stable triazole. Different linker lengths and types (alkyl vs PEG-like) were installed to elucidate the optimal linker for binding, reaction with a tag, and considering the overall solubility of the ligand.

Synthesis. Imide **4**, prepared according to a literature[25] method, was alkylated using either bromobutane or bromopropane to give **5** or the previously reported **6**[25] (Scheme 1). The vinyl amine of substituted imidamides **5** and **6** was hydrolyzed to give **7** and **8**, respectively, which was then nitrated and reduced to afford diamines **9** and **10**, respectively, in moderate yield. With the 2,4-dimethoxybenzyl (DMB) protecting group in place, diamines **9** and **10** were coupled with bicyclo[2.2.2]-octane-1,4-dicarboxylic acid monomethyl ester using *O*-(7-azabenzotriazol-1-yl)-*N*,*N*,*N*′,*N*′-tetramethyluronium hexafluorophosphate (HATU) to give the monoamidated product, which subsequently underwent dehydrative ring closure and methyl ester hydrolysis using KOH in isopropanol at reflux to give carboxylic acids **11** and **12**. The carboxylic acid was then either methylated to give **13** or coupled via HATU-mediated amide bond formation with a series of amino linkers containing a terminal azide or alkyne to give **14**−**21**.

The DMB group of **13**−**21** was removed, and the imide alkylated using <1 equiv of an alkyl bromide at room temperature to give **UODC2**, **UODC5**, **UODC6**, and **UODC9**−**UODC14** (Scheme 1). In all instances, one regioisomer was produced, with alkylation of the imidazole not detected. Potentially covalent sulfonyl fluorides **UODC6** and **UODC2** were converted to sulfonic acids **UODC7** and **UODC3**, respectively, to allow comparison to analogues without covalent capacity. Initially for all compounds, the imidazole -NH was protected with a pivaloyloxymethyl (POM) group but eventual removal of POM with a sulfonyl fluoride present proved to be troublesome with high conversion to the sulfonic acid occurring under most conditions. To synthesize the analogues without the sulfonyl fluoride "covalent arm", the imidazole -NH of **14** and **15** was first protected with POM to give **22** and **23**, respectively, followed by DMB cleavage and reaction with >1 equiv of bromopropane at 50 °C to give **24** and

https://doi.org/10.1021/acs.jmedchem.0c02169
J. Med. Chem. 2021, 64, 8161−8178

Scheme 1[a]

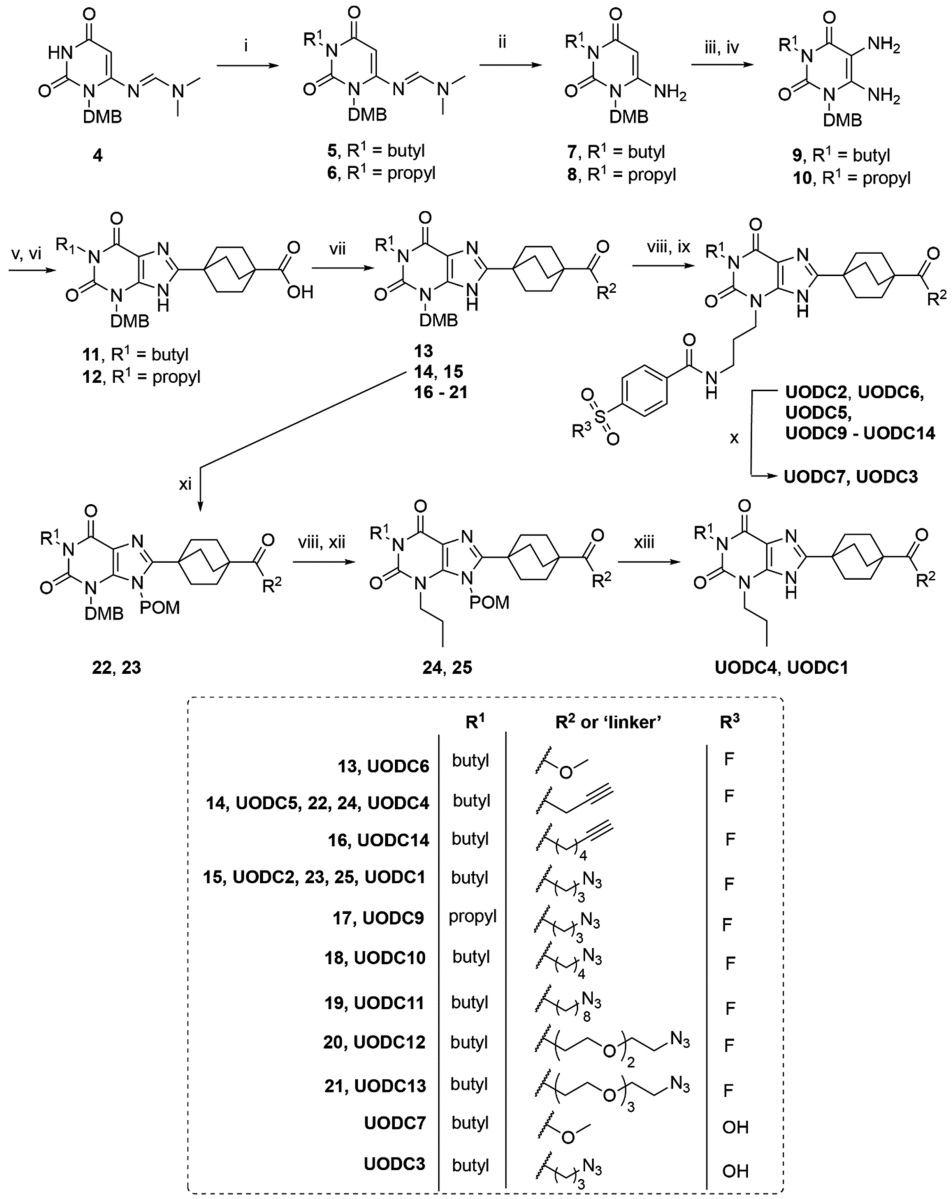

[a]Reagents and conditions: (i) R^1-Br, Cs_2CO_3, TBAB, ACN, DMF, 60 °C, 3 h, 76−80%; (ii) 2 M KOH, MeOH, 50 °C, 1 h, 84−88%; (iii) $NaNO_2$, 50% AcOH, 70 °C, 1 h; (iv) $Na_2S_2O_4$, 25% aq. NH_4OH, MeOH, 80 °C, 4 h, 62−76% (over two steps); (v) bicyclo[2.2.2]octane-1,4-dicarboxylic acid monomethyl ester, HATU, NEt_3, ACN, 1 h, rt; (vi) 1 M KOH, *i*-PrOH, reflux, 1 h, 59−73% (over two steps); (vii) H_2SO_4, MeOH, reflux, 3 h, 71%, or NH_2- "linker" (see the Supporting Information), HATU, DIPEA, DMF, 18 h, rt, 42−98%; (viii) TFA, 50 °C; (ix) 4-[(3-bromopropyl)carbamoyl]benzene-1-sulfonyl fluoride (see the Supporting Information), K_2CO_3, DMF, rt, 11−98% (over two steps); (x) 1 M NaOH, MeOH, rt, 1 h, 88−95%; (xi) POM-Cl, K_2CO_3, DMF, 50 °C, 18 h, 52−57%; (xii) bromopropane, K_2CO_3, DMF, 50 °C, 18 h, 42−77%; (xiii) 2 M NaOH, MeOH, rt, 1 h, 89−98%.

25, respectively. Finally, **UODC4** and **UODC1** were obtained upon removal of the POM group with methanolic NaOH. One example of a cyclohexyl moiety in place of the bicyclo-octyl was synthesized using analogous reaction conditions to give **UODC8** (Scheme 2), the only difference to DU172 being an N1-butyl instead of a propyl.

Pharmacology. We first determined the apparent affinity of newly synthesized compounds for the hA_1R in membranes derived from A_1R-FlpInCHO cells, based on displacement of the antagonist radioligand, [^{3}H]DPCPX (1 nM). All compounds, except for **UODC8**, completely displaced the binding of [^{3}H]DPCPX, indicating a competitive interaction for the orthosteric site (Figure 2 and Figure S1); the estimated affinities are listed in Table 1. The effect of **UODC8** was bell-shaped, completely displacing [^{3}H]DPCPX binding up to 1 μM; however, at 10 μM, less displacement was observed. This bell-shaped inhibition curve may indicate a bitopic mode of action[26] or alternatively nonspecific effects or a lack of solubility at 10 μM. Thus, **UODC8** was empirically fitted to a one-site inhibition mass action curve, except at 10 μM, to estimate affinity. The bicyclo[2.2.2]octyl variant of **UODC8**, **UODC6**, had a similar affinity for the A_1R, whereas substituting the sulfonyl fluoride for sulfonic acid (**UODC7**) decreased the affinity ~10-fold. Given that incorporation of the sulfonyl

https://doi.org/10.1021/acs.jmedchem.0c02169
J. Med. Chem. 2021, 64, 8161−8178

Scheme 2[a]

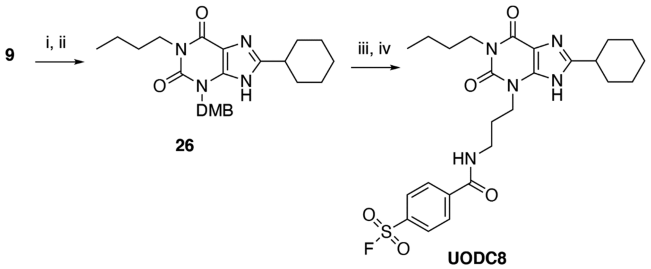

[a]Reagents and conditions: (i) cyclohexanoic acid, HATU, NEt_3, ACN, rt, 1 h; (ii) 1 N KOH, *i*-PrOH, reflux, 1 h, 88% (over two steps); (iii) TFA, 50 °C; (iv) 4-[(3-bromopropyl)carbamoyl]-benzene-1-sulfonyl fluoride, K_2CO_3, DMF, rt, 18 h, 63% (over two steps).

fluoride warhead was tolerated, we next tested the impact of incorporating an azide clickable handle to replace the ethyl dimethylamine of **3** to generate the bifunctional probe, **UODC2**, which had a high A_1R affinity (sub-10 nM) equivalent to that reported for **3** (K_i = 6 nM hA_1R). Notably, the reversible sulfonic acid variant, **UODC3**, had an ~100-fold lower affinity compared to that of **UODC2**. With regard to the N1 substituent, the N1-propyl xanthine (**UODC9**) had the same affinity relative to that of N1-butyl (**UODC2**). Similarly, extending the azide linker length to C4 (**UODC10**) or C8 (**UODC11**) or replacing the carbon chain with a PEG2 (**UODC12**) or PEG3 (**UODC13**) linker had little effect on affinity with the value for each compound being within 2-fold of that of **UODC2**. We next sought to establish the tolerability of an alternative clickable handle. Introducing a terminal alkyne to give **UODC4** resulted in 10-fold reduced affinity when compared to that of the azido equivalent (**UODC1**). Installing a terminal alkyne with the sulfonyl fluoride warhead (**UODC5**) yielded a bifunctional probe with good affinity, albeit 3-fold lower than that of **UODC2**. Extending the linker between the amine and the terminal alkyne to C4 resulted in the highest-affinity bifunctional A_1R probe (**UODC14**). UODC14 had a similar affinity (within 3-fold) for the A_1R when compared with that of the previously reported DU172 (**1**).[22] Overall, it was pleasing that the previously reported xanthine N3-sulfonyl fluoride terminating substituent[22,27] was well tolerated on the **UODC** bifunctional probes containing the C8-bicyclo[2.2.2]octyl clickable linkers.

We next sought to test if each probe retained A_1R antagonist properties. The A_1R preferentially couples to $G_{i/o}$ proteins, resulting in adenylate cyclase inhibition and thereby reducing cyclic adenosine monophosphate (cAMP) production. Thus, we used the A_1R-mediated inhibition of forskolin-stimulated cAMP accumulation assays in A_1R-FlpInCHO cells to test biological effects. Concentration−response curves for the nonselective agonist NECA were generated in the absence and presence of each compound at 1 μM (Figure 2 and Figure S1). Each compound caused a rightward shift of the NECA curve, with no suppression of the maximal response, consistent with each compound acting as a competitive A_1R antagonist. Analysis of these data yielded functional affinity estimates (pK_b) that were in good agreement with pK_i estimates from radioligand binding

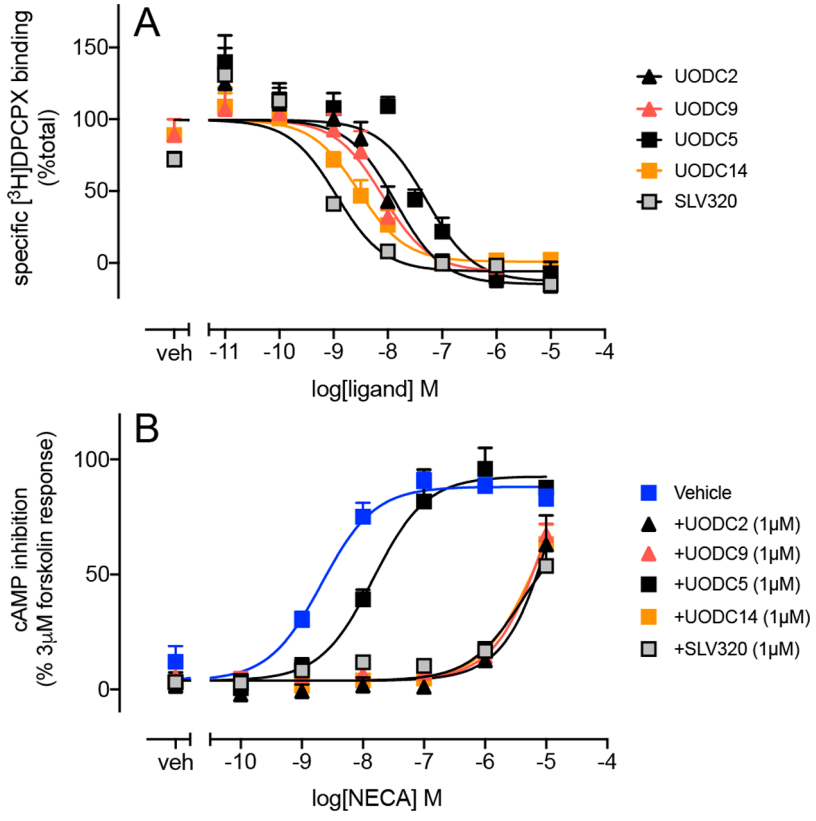

Figure 2. Pharmacological characterization of synthesized compounds in radioligand binding and cAMP inhibition assays. (A) Inhibition of binding of [^{3}H]DPCPX to membrane preparations from FlpInCHO-hA_1R. (B) NECA concentration−response curves for cAMP inhibition in the absence or presence of test compounds (1 μM) and SLV320 (1 μM) in FlpInCHO-hA_1R cells. Data represent means ± SEM from at least three experiments performed in duplicate (see Table 1 for exact numbers). Error bars not shown lie within the dimensions of the symbol.

https://doi.org/10.1021/acs.jmedchem.0c02169
J. Med. Chem. 2021, 64, 8161−8178

Table 1. Affinity Estimates (pK_i and pK_B) of Test Compounds from [^{3}H]DPCPX Competition Binding and cAMP Inhibition Assays, Respectively, in FlpInCHO-hA_1R Cells[a]

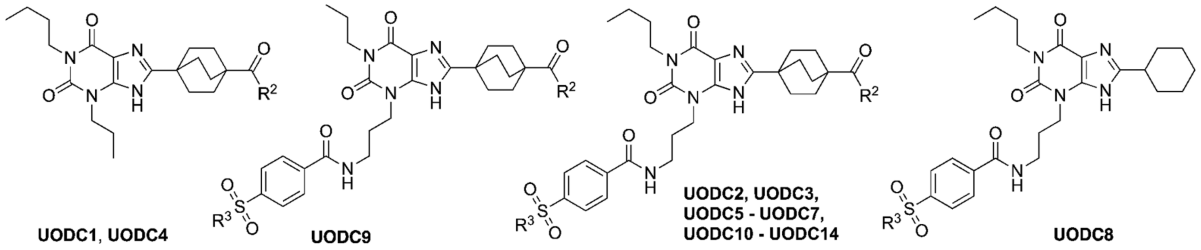

Compound	R^2	R^3	[^{3}H] DPCPX competition binding				cAMP inhibition	
			pK_i[b] (nM)	*n*	pK_i[b] (nM) - post washout	*n*	pK_b[c] (nM)	*n*
SLV320	-	-	9.25 ± 0.08 (0.6)	6	n/a		9.27 ± 0.14 (0.5)	6
UODC8	-	F	7.92 ± 0.33 (12.1)	4	n/a		7.59 ± 0.30 (26.0)	6
UODC6		F	7.76 ± 0.11 (17.3)	4	7.05 ± 0.11 (89.3)	9	7.77 ± 0.26 (17.1)	5
UODC7		OH	6.75 ± 0.40 (179)	4	n/d		7.04 ± 0.10 (92.0)	5
UODC1	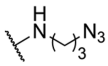	-	8.27 ± 0.08 (5.4)	4	6.09 ± 0.32 (805)	3	8.47 ± 0.26 (3.4)	4
UODC2	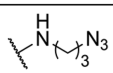	F	8.17 ± 0.14 (6.7)	6	8.19 ± 0.11 (6.5)	7	9.31 ± 0.16 (0.5)	4
UODC3	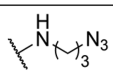	OH	6.22 ± 0.11 (605)	3	n/d		7.06 ± 0.13 (87.5)	4
UODC9	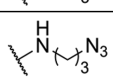	F	8.46 ± 0.15 (3.5)	4	8.11 ± 0.07 (7.8)	4	9.19 ± 0.13 (0.6)	6
UODC10	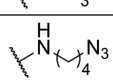	F	7.84 ± 0.31 (14.4)	4	7.24 ± 0.15 (58.1)	3	8.28 ± 0.31 (5.2)	6
UODC11	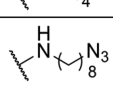	F	8.43 ± 0.18 (3.7)	4	7.79 ± 0.10 (16.1)	3	8.62 ± 0.17 (2.4)	6
UODC12	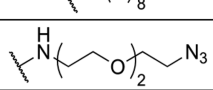	F	8.22 ± 0.13 (6.1)	4	8.00 ± 0.05 (10.0)	5	8.86 ± 0.06 (1.4)	6
UODC13	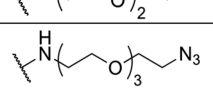	F	8.30 ± 0.16 (5.0)	4	7.86 ± 0.08 (13.9)	5	8.65 ± 0.13 (2.2)	6
UODC4	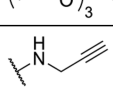	-	7.36 ± 0.06 (43.4)	4	6.14 ± 0.12 (731)	3	7.04 ± 0.30 (91.0)	5
UODC5	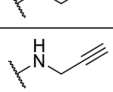	F	7.58 ± 0.11 (26.1)	6	7.41 ± 0.09 (38.8)	7	6.23 ± 0.39 (585)	5
UODC14	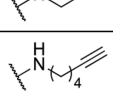	F	8.81 ± 0.24 (1.6)	4	8.03 ± 0.28 (9.3)	5	9.20 ± 0.22 (0.6)	6

[a]Data are expressed as means ± SEM from the indicated number (*n*) of independent experiments performed in duplicate. n/a denotes not available, and n/d denotes not determined. [b]Negative logarithm of the equilibrium dissociation constant for antagonists determined from displacement of [^{3}H]DPCPX binding using the Cheng−Prusoff equation. [c]Negative logarithm of the equilibrium dissociation constant for antagonists as determined from NECA concentration−response curves for cAMP inhibition in the absence and presence of the indicated compound added 5 min prior to NECA addition using the Gaddum−Schild equations, assuming a Schild slope.

assays (Table 1). A high affinity is desirable for covalent clickable probes, as it allows sufficient receptor occupancy to ensure negligible interactions with other unrelated targets.

To ascertain the irreversible interaction of sulfonyl fluoride-containing antagonists (after incubation for 3 h), radioligand displacement assays were performed following extensive washout (6 × 20 min).[19,27] Preincubation with compounds containing a sulfonyl fluoride warhead (e.g., **UODC2**, **UODC5**, **UODC6**, **UODC9**, and **UODC14**) completely abolished [^{3}H]DPCPX binding after the washing cycles, suggesting

https://doi.org/10.1021/acs.jmedchem.0c02169
J. Med. Chem. 2021, 64, 8161−8178

covalent and irreversible binding to the A_1R (representatives shown in Figure 3, and all other covalent compounds are reported in Figure S2 and Table 1). Importantly, under the same conditions, preincubation with sulfonic acid-containing compounds **UODC3** and **UODC7**, followed by washout, did not displace the radioligand, demonstrating the extensive washout steps successfully removed noncovalent compounds. In addition, affinity estimates for sulfonyl fluoride-containing compounds were unchanged with washout, suggesting the extensive washing did not damage the membrane integrity or alter membrane binding sites.

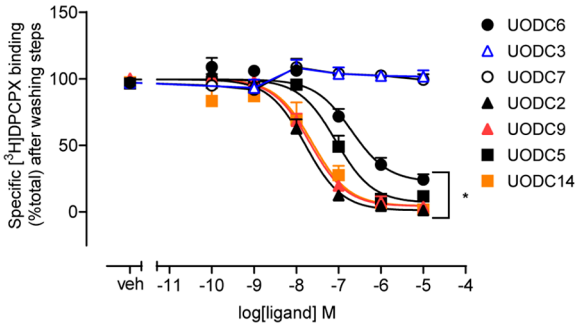

Figure 3. A_1R clickable ligands with the fluorosulfonyl warhead irreversibly bind to the hA_1R. [^{3}H]DPCPX binding after preincubation with increasing concentrations of test compounds followed by a 6 × 20 min washout. Experiments were performed with fluorosulfonyl-containing ligands that bind irreversibly (**UODC2**, **UODC5**, **UODC6**, **UODC9**, and **UODC14**) as well as sulfonic acid-containing ligands that were reversible (**UODC3** and **UODC7**). Data represent the mean ± SEM from at least three experiments performed in duplicate (see Table 1 for exact numbers). Error bars not shown lie within the dimensions of the symbol. *p < 0.0001, from one-way analysis of variance with Dunnett's post-test compared to vehicle.

Subsequently, we tested sulfonyl fluoride-containing clickable antagonists **UODC2**, **UODC5**, and **UODC9**–**UODC14** for selectivity against the other adenosine receptor subtypes ($A_{2A}R$, $A_{2B}R$, and A_3R). For this purpose, we employed a functional response common to all four subtypes, namely, cAMP accumulation, which is inhibited by the A_1R and A_3R but stimulated by the $A_{2A}R$ and $A_{2B}R$. Concentration–response curves were generated in the absence or presence of a submaximal EC_{80} concentration of NECA in parallel with a reference selective antagonist for each subtype. With the exception of **UODC5** at the $A_{2A}R$ and $A_{2B}R$, all compounds inhibited the NECA response (Figure 4 and Figure S3). In general, all compounds had similar affinity (within 3-fold) for the A_1R and A_3R (Table 2), the exception being **UODC14**, which had a 10-fold higher affinity for the A_1R than for the A_3R. This was surprising given the excellent A_1R over A_3R selectivity exhibited by previously reported bicyclo[2.2.2]octyl 1,3-dipropylxanthine derivatives (e.g., compounds **17**–**22** in ref 24). However, an important difference is that our bicyclo[2.2.2]-octyl xanthines contain a covalent warhead. Therefore, given the similarly located Tyr in the A_1R and A_3R (Figure 5 and discussed below), the covalent nature of these ligands may in part confer A_3R affinity. In addition, selectivity assessment of noncovalent derivatives **UODC1** and **UODC4** also contradicted the earlier SAR report, which relied on radioligand binding rather than functional responses to determine the selectivity of bicyclo[2.2.2]octyl xanthines.[24] Importantly, each ligand showed an ∼10-fold greater affinity for the A_1R than for both the $A_{2A}R$ and the $A_{2B}R$ (Table 2). The superior affinity of the **UODC** ligands for the A_1R and A_3R over the $A_{2A}R$ and $A_{2B}R$ is in line with a previous xanthine SAR, in that longer alkyl and

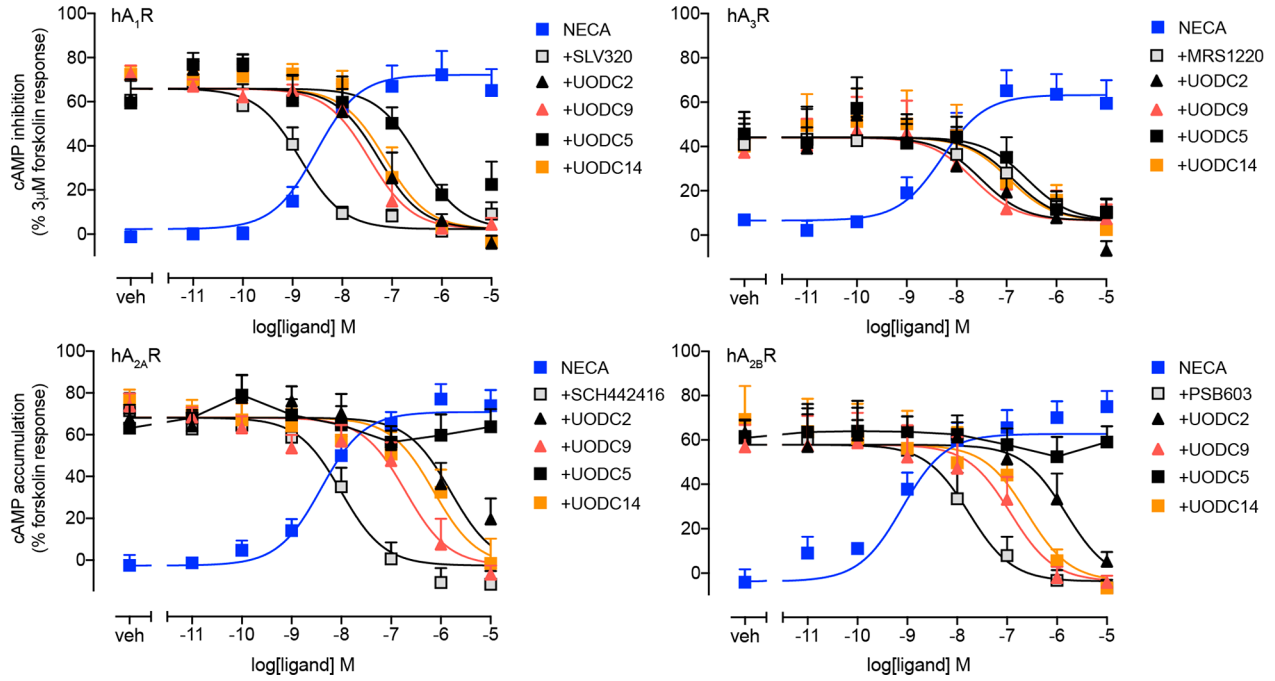

Figure 4. Adenosine receptor subtype selectivity of A_1R antagonists, bearing a click handle (i.e., terminal alkyne and aliphatic azide) and fluorosulfonyl warhead. Functional cAMP concentration–response curves for NECA (blue line) or A_1R antagonists in the presence of a submaximal (EC_{80}) NECA concentration at the indicated AR subtype stably expressed in FlpInCHO cells. Selective antagonists SLV320, SCH442416, PSB603, and MRS1220 for the A_1R, $A_{2A}R$, $A_{2B}R$, and A_3R, respectively, were used in parallel as positive controls. Data represent means ± SEM from at least three experiments performed in duplicate (see Table 2 for exact numbers). Error bars not shown lie within the dimensions of the symbol.

https://doi.org/10.1021/acs.jmedchem.0c02169
J. Med. Chem. 2021, 64, 8161–8178

Table 2. Adenosine Receptor Subtype Affinity (pK_B) Values of Selected Test Compounds on cAMP Inhibition and Accumulation in Human AR-Expressing FlpInCHO Cells[a]

	hA_1R		$hA_{2A}R$		$hA_{2B}R$		hA_3R	
	pK_B (nM)	*n*	pK_B (nM)	*n*	pK_B (nM)	*n*	pK_B (nM)	*n*
UODC2	8.09 ± 0.31 (8.1)	8	7.42 ± 0.25 (38.0)	7	7.10 ± 0.15 (79.4)	8	8.38 ± 0.17 (4.2)	13
UODC9	8.56 ± 0.21 (2.8)	4	7.58 ± 0.19 (26.3)	5	7.75 ± 0.26 (17.8)	4	7.96 ± 0.51 (11.0)	6
UODC10	8.41 ± 0.13 (3.9)	4	6.78 ± 0.31 (166)	5	7.58 ± 0.70 (26.3)	4	8.31 ± 0.50 (4.9)	6
UODC11	7.99 ± 0.19 (10.2)	4	nd	5	8.17 ± 0.68 (6.7)	4	8.52 ± 0.50 (3.0)	5
UODC12	8.45 ± 0.18 (3.5)	4	7.50 ± 0.26 (31.6)	5	7.64 ± 0.59 (22.9)	4	7.40 ± 0.35 (39.8)	7
UODC13	8.48 ± 0.16 (3.3)	4	7.44 ± 0.34 (36.3)	5	7.02 ± 0.15 (95.5)	4	8.08 ± 0.13 (8.3)	6
UODC5	7.51 ± 0.16 (30.9)	7	nd	9	nd	8	7.33 ± 0.18 (46.8)	12
UODC14	8.41 ± 0.17 (3.9)	5	7.15 ± 0.28 (70.8)	5	7.45 ± 0.12 (35.4)	4	7.36 ± 0.38 (43.7)	7
UODC1	8.40 ± 0.32	7	nd	7	7.73 ± 0.14	7	8.13 ± 0.29	12
UODC4	7.01 ± 0.66	4	nd	6	nd	6	7.45 ± 0.36	6
reference antagonist[b]	9.44 ± 0.43 (0.4)	8	9.47 ± 0.20 (0.3)	9	8.87 ± 0.23 (1.3)	8	8.30 ± 0.34 (5.0)	11

[a]Data are expressed as means ± SEM from the indicated number (*n*) of independent experiments performed in duplicate. nd denotes not defined due to incomplete inhibition and a poor curve fit. [b]SLV320, SCH442416, PSB603, and MRS1220 were used as reference antagonists in A_1R-, $A_{2A}R$, $A_{2B}R$-, and A_3R-FlpInCHO cells, respectively.

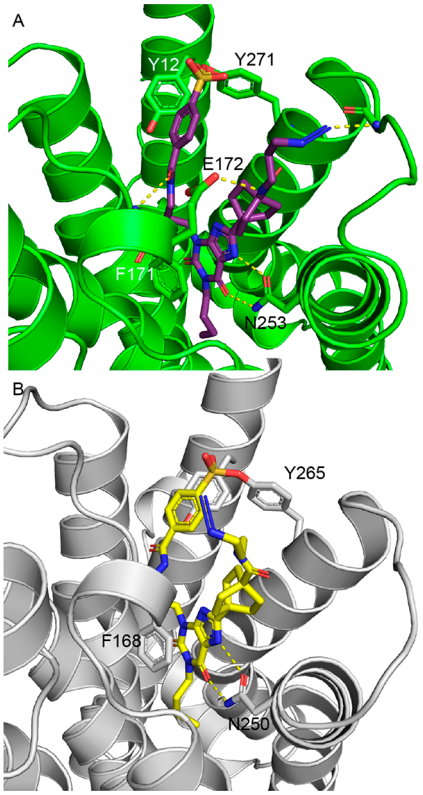

Figure 5. Binding of **UODC2** in (A) the crystal structure of the A_1R (PDB entry 5UEN) and (B) the homology model of the A_3R. The A_1R is shown as a green ribbon, A_3R as a white ribbon, and **UODC2** as purple and yellow sticks. Dashed yellow lines indicate hydrogen bonds. **UODC2** was docked covalently to Y271 and Y265.

bulkier moieties can tolerated at the N1 and N3 positions of the A_1R and A_3R but not at those of the $A_{2A}R$ and $A_{2B}R$ (as discussed by Cheng et al.[23]). During ligand design, we hypothesized that a xanthine N1-butyl (as opposed to propyl) alkyl chain might imbue better A_1R selectivity over the other AR subtypes. However, comparison between the one N1-propyl derivative (**UODC9**) and the equivalent N1-butyl derivative (**UODC2**) revealed little difference in activity across all AR subtypes (Table 2).

Molecular Modeling. Compound **UODC2** was docked into the A_1R crystal structure (PDB entry 5UEN)[22] using a covalent linkage to $Y271^{7.36}$. **UODC2** binds to the A_1R in a fashion similar to that of DU172 (five of the top six poses out of 10) with hydrogen bonds between $N253^{6.55}$ and the xanthine scaffold. A new hydrogen bond is formed with $F171^{EL2}$ via the amide carbonyl oxygen where the amide is flipped compared with DU172 (Figure 5). The flexible terminal azide linker of **UODC2** was easily accommodated and oriented toward the extracellular space, with hydrogen bonds seen between the azide and the main chain carbonyl of $K265^{EL3}$. Some variation exists between poses in the flexible propylazido chain, which is to be expected.

UODC2 was also docked into an A_3R homology model (using the A_1R crystal structure, PDB entry 5UEN, as a template) using a covalent linkage to $Y265^{7.36}$. The top-ranked pose is similar to that of DU172 in the A_1R crystal structure (Figure 5), when superimposed. A small cluster of three poses shows the xanthine ring shifted toward a more central position; however, these poses score much lower than the top-ranked pose and appear to have close contacts between the phenyl ring of the covalent arm and the bicyclo-octyl moiety. A key hydrogen bonding interaction between $N250^{6.55}$ and the xanthine scaffold was maintained in the A_3R along with π-interactions with $F168^{EL2}$. Indeed, Yang et al.[28] recently identified $Y265^{7.36}$ forming a covalent bond with the fluorosulfonyl warhead of their compound "**17b**", which is structurally related to **UODC2**, albeit with an ∼10-fold lower affinity for the A_3R when compared to that of **UODC2**. Residue $Y265^{7.36}$ of the A_3R is in the same position as $Y271^{7.36}$ in the A_1R; therefore, **UODC2** and related compounds could covalently bind to the A_3R, as well. Studies of the docking of **UODC9** and **UODC14** to the A_3R showed both compounds could be accommodated within the orthosteric site (data not shown). An equivalently positioned Tyr is also present in the $A_{2A}R$ (Y271)[29] but not in the $A_{2B}R$.[30] A potential reason for the ∼10-fold greater affinity for ligands reported herein for the A_1R over the $A_{2A}R$ and $A_{2B}R$ could be that both the $A_{2A}R$ and the $A_{2B}R$ contain a Met residue ($M270^{7.35}$ and $M272^{7.35}$, respectively) in the position occupied by $T270^{7.35}$ in the A_1R and $L264^{7.35}$ in the A_3R, leading to Met−cyclooctyl steric clashes. Docking of **UODC2** to the $A_{2A}R$ (PDB entry 6LPK)[31] under the same covalent conditions produced no poses binding in the orthosteric site (Figure S4).

https://doi.org/10.1021/acs.jmedchem.0c02169
J. Med. Chem. 2021, 64, 8161−8178

Given the high affinity for the A_3R, we assessed the potential for our covalent clickable compounds to irreversibly bind to the hA_3R. For this purpose, we performed a NanoBRET displacement assay in transiently transfected NLuc-tagged A_3R-HEK293A cells using a washout protocol similar to that used for the hA_1R (Figure 3). Antagonists **UODC2**, **UODC6**, **UODC5**, and **UODC14** weakened the binding of the fluorescent antagonist CA200645 measured by resonance energy transfer, while sulfonic acid analogues **UODC3** and **UODC7** were completely washed away (Figure 6). As such, our

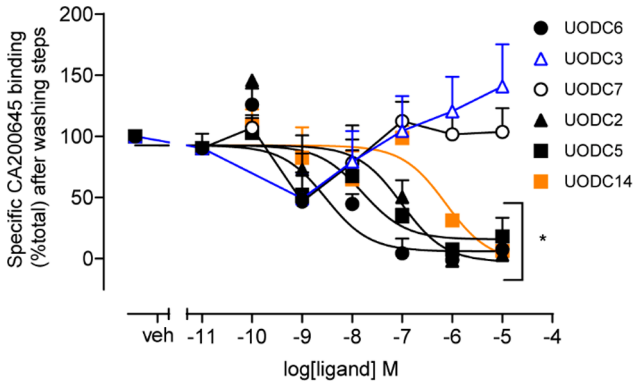

Figure 6. Antagonists with a sulfonyl fluoride warhead irreversibly bind to hA_3R. Inhibition of CA200645 binding in HEK293A cells transiently transfected with the Nluc-tagged A_3R. Competition binding after preincubation for 3 h with a 6 × 20 min washout. Data represent means ± SEM from at least three experiments performed in duplicate. *p < 0.01, one-way analysis of variance with Dunnett's post-test compared to the vehicle.

covalent clickable antagonists may be useful tools for hA_3R structural elucidation, particularly given high-resolution structures that are currently lacking for the A_3R. Furthermore, despite our clickable probes having high affinities for the A_1R and A_3R, their impact remains high with respect to visualizing receptor subcellular distribution and trafficking in recombinant and native cells. The A_1R and A_3R have differential tissue expression; the A_1R is strongly expressed in the cerebral cortex, heart, parathyroid gland, and pancreas, whereas the A_3R is strongly expressed in granulocytes as per the Human Protein Atlas (http://www.proteinatlas.org).[32]

Fluorescent Labeling of the hA_1R. Having established the selectivity and covalent binding properties of our novel A_1R ligands, we next sought to confirm the clickability of two azide-containing (**UODC2** and **UODC9**) and two alkyne-containing (**UODC5** and **UODC14**) probes. To accomplish this task, A_1R-FlpInCHO cells were preincubated with increasing concentrations of probes to allow covalent binding, followed by click chemistry to attach a complementary clickable near-infrared fluorophore, either Cy5.5-azide or Cy5.5-alkyne. Upon cell lysis, probe-labeled proteins were separated by SDS−PAGE, and fluorescence was visualized and immunoblotting performed to detect A_1R via a C-terminal V5 epitope tag (Figure 7). In the absence of clickable probes, there was little Cy5.5 incorporation in A_1R-FlpInCHO cells. Concentration-dependent click chemistry incorporation of Cy5.5 was observed in the presence of **UODC2**, **UODC9**, and **UODC14**, but not **UODC5**, suggesting a longer linker than N-propargyl is required to facilitate the attachment of the fluorophore. Importantly, multiple bands were evident with molecular weights ranging from 37 to 50 kDa in both Cy5.5 labeling and immunoblotting. The specificity of the anti-V5 antibody was assessed in nontransfected FlpIn CHO cells (Figure S5), which confirmed these apparent bands are A_1R-specific fluorescent signals. As noted previously for the CB_2R[20] and $A_{2A}R$,[21] these multiple bands likely represent different post-translationally modified receptors. To demonstrate the specificity of the affinity-based probes, we investigated whether a competitive antagonist could inhibit labeling. A_1R-FlpInCHO cells were preincubated with a saturating concentration (10 μM) of the irreversible competitor, **UODC6**, prior to labeling and click chemistry to incorporate Cy5.5. In the presence of **UODC6**, there was minimal Cy5.5 incorporation, indicating the binding of each bifunctional probe was specifically blocked (Figure 8). Similarly, there was no labeling of nontransfected FlpInCHO cells in the presence of any of the clickable probes (Figure 8). Collectively, these results show that bifunctional compounds **UODC2**, **UODC9**, and **UODC14** can be employed as affinity-based clickable probes for the A_1R.

CONCLUSION

In summary, we report the rational design and validation of bifunctional A_1R and A_3R orthosteric antagonists that are both covalent and clickable. The bicyclo[2.2.2]octyl xanthine-based scaffold used herein showed similar affinity (within 3-fold) for the A_1R and A_3R, with moderate selectivity over $A_{2A}R$ and $A_{2B}R$ subtypes. The fluorosulfonyl moiety is predicted to form a covalent bond with a $Tyr^{7.36}$ at the top of TM7, which is conserved between the A_1R and A_3R. Once bound to the receptor, compounds **UODC2**, **UODC9**, and **UODC14** were conjugated via click chemistry with a fluorophore. By preincubation with a competitive ligand, we demonstrate that probe-dependent labeling of the A_1R was inhibited. Therefore, we propose that these first clickable and covalent A_1R/A_3R orthosteric antagonists present new tools to aid in the structural determination of the A_3R, as well as receptor localization in recombinant and native systems in which the A_1R and A_3R are differentially expressed.

EXPERIMENTAL SECTION

Chemistry. Chemicals were purchased from Sigma-Aldrich, AK Scientific, Alfa Aesar, or Merck and used without further purification. Unless otherwise stated, anhydrous solvents and dry atmospheric conditions were used in all reactions. Unless otherwise stated, all reactions were carried out at room temperature (rt) under atmospheric pressure. Thin layer chromatography (TLC) was carried out on silica gel plates 60 F_{254} and visualized under UV light at 254 nm. Potassium permanganate dip was used to visualize non-UV active compounds. Flash column chromatography separations using 40−63 μm silica were performed by the gradient elution method, and the elution solvent system is given in each instance. Reverse-phase high-performance liquid chromatography (RP-HPLC) was carried out on an Agilent 1260 Infinity system, using a YMC-C8 5 μm (150 mm × 10 mm) column at a rate of 3 mL/min for semipreparative RP-HPLC and a YMC-C8 5 μm (150 mm × 4.6 mm) column at a rate of 1 mL/min for analytical RP-HPLC. The following mobile phases were used A, H_2O (0.05% TFA), and B, 9:1 ACN/H_2O (0.05% TFA). The standard analytical method for analytical RP-HPLC (for which retention times of compounds are given) was 5% B for 1 min and a linear gradient from 5% to 95% B from 1 to 27 min (followed by a 1 min hold at 95% B and then a 2 min linear gradient from 95% to 5% B and a 4 min re-equilibration at 5% B). All final compounds were >95% RP-HPLC analytically pure as assessed by peak integration at 245 nm. A typical semipreparative HPLC method was carried out as described: 5% B for 1 min and a linear gradient from 5% to 95% B from 1 to 12 min (followed by a 2 min hold at 95% B and then a 3 min linear gradient from 95% to 5%). High-resolution electrospray ionization mass spectra (HRMS-ESI) were recorded on a

https://doi.org/10.1021/acs.jmedchem.0c02169
J. Med. Chem. 2021, 64, 8161−8178

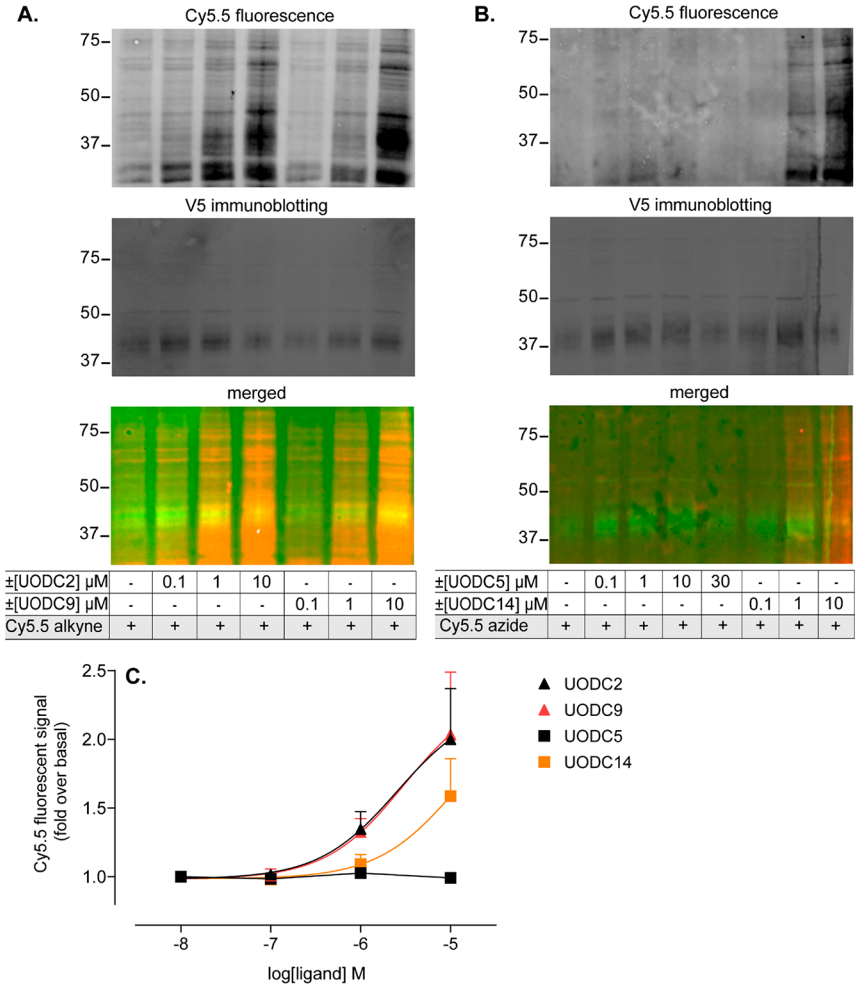

Figure 7. Concentration-dependent incorporation of Cy5.5 is evident in hA$_1$R-FlpIn CHO cells by **UODC2**, **UODC9**, and **UODC14** but not **UODC5**. (A and B) Representative in-gel Cy5.5 fluorescence images coupled with immunoblots for V5 (indicative of the A$_1$R) shown in gray scale and merged Cy5.5 fluorescence in red and anti-V5 in green. (C) Quantification of fluorescence intensity labeled with increasing concentrations of clickable probes. Cy5.5 fluorescence was corrected for relative A$_1$R level (based on V5 immunoblotting against the C-terminal V5 epitope tag), expressed as fold over basal. Data represent means ± SEM from three experiments. Error bars not shown lie within the dimensions of the symbol.

microTOF$_Q$ mass spectrometer. Proton (^{1}H), fluorine (^{19}F), and carbon (^{13}C) nuclear magnetic resonance (NMR) spectroscopy was carried out using a 400 or 500 MHz Varian NMR spectrometer. Two-dimensional NMR experiments, including COSY, HSQC, HMBC, and NOESY, were used to assign chemical shifts and for some compounds to assign a regioisomer. Chemical shifts are listed on the δ scale in parts per million, referenced to $CDCl_3$ (^{1}H NMR δ 7.26; ^{13}C NMR δ 77.16) or DMSO-d_6 (^{1}H NMR δ 2.50; ^{13}C NMR δ 39.52) with residual solvent as the internal standard and coupling constants (J) recorded in hertz. Note that not all magnetically non-equivalent carbons were observed in the ^{13}C NMR spectrum for all compounds. Signal multiplicities are assigned as follows: s, singlet; d, doublet; t, triplet; q, quartet; dd, doublet of doublets; br, broad; m, multiplet.

General Procedure for the Alkylation of 4. To a stirred suspension of **4** in acetonitrile and DMF were added Cs_2CO_3 and tetra-*N*-butylammonium bromide (TBAB). The bromoalkane was added dropwise over 15 min, and the reaction mixture was stirred for 1 h at rt and then for 3 h at 60 °C. Ice−water was added, and the mixture was stirred for 30 min. The mixture was extracted with CH_2Cl_2 and washed with saturated aqueous $NaHCO_3$ and brine. The pooled organic layers were dried with $MgSO_4$, filtered, and concentrated *in vacuo*. The solid obtained was recrystallized with 50% aqueous methanol, filtered, washed with cold 50% aqueous methanol, and air-dried.

*N′-{1-Butyl-3-[(2,4-dimethylphenyl)methyl]-2,6-dioxo-1,2,3,6-tetrahydropyrimidin-4-yl}-N,N-dimethylmethanimidamide (**5**).* **4** (3.10 g, 9.32 mmol), acetonitrile (11 mL), DMF (6 mL), Cs_2CO_3 (3.25 g, 9.97 mmol), TBAB (20 mg, 0.06 mmol), and 1-bromobutane (1.91 g, 1.51 mL, 13.93 mmol) gave **5** (2.75 g, 7.08 mmol, 76%) as off-white crystals. ^{1}H NMR (400 MHz, DMSO-d_6): δ 0.88 (t, J = 7.4 Hz, 3H), 1.25 (m, 2H), 1.47 (m, 2H), 2.83 (s, 3H), 3.04 (s, 3H), 3.71 (s, 3H), 3.76 (t, J = 7.2 Hz, 2H), 3.78 (s, 3H), 5.05 (s, 2H), 5.17 (s, 1H), 6.41 (dd, J = 2.4, 8.4 Hz, 1H), 6.53 (d, J = 2.4 Hz, 1H), 6.64 (d, J = 8.4 Hz, 1H), 8.04 (s, 1H). ^{13}C NMR (400 MHz, DMSO-d_6): δ 13.72, 19.64, 29.60, 34.13, 39.46, 39.73, 39.92, 55.11, 55.35, 81.79, 98.13, 104.39, 118.19, 126.22, 151.77, 155.82, 157.03, 158.94, 159.20, 162.05. HRMS (ESI) calcd for $C_{20}H_{29}N_4O_4^+$ [M + H]$^+$ m/z 389.2183 and $C_{20}H_{28}N_4NaO_4^+$ [M + Na]$^+$ m/z 411.2003, found m/z 389.2168 and 411.1981.

*N′-{3-[(2,4-Dimethylphenyl)methyl]-2,6-dioxo-1-propyl-1,2,3,6-tetrahydropyrimidin-4-yl}-N,N-dimethylmethanimidamide (**6**).* **4** (1.00 g, 3.00 mmol), acetonitrile (3.5 mL), DMF (2 mL), Cs_2CO_3 (1.08 g, 3.30 mmol), TBAB (97 mg, 0.30 mmol), and 1-bromopropane (0.56 g, 0.41 mL, 4.51 mmol) gave **6** (0.93 g, 2.39 mmol, 80%) as off-white crystals. ^{1}H NMR (400 MHz, DMSO-d_6): δ 0.83 (t, J = 7.2 Hz, 3H), 1.51 (m, 2H), 2.83 (s, 3H), 3.04 (s, 3H), 3.71 (s, 3H), 3.72 (t, J = 7.2 Hz, 2H), 3.78 (s, 3H), 5.05 (s, 2H), 5.17 (s, 1H), 6.41 (dd, J = 2.4, 8.4 Hz, 1H), 6.53 (d, J = 2.4 Hz, 1H), 6.64 (d, J = 8.4 Hz, 1H), 8.04 (s, 1H). ^{13}C NMR (400 MHz, DMSO-d_6): δ 11.19, 20.78, 34.15, 40.01, 40.20, 41.51, 55.12, 55.37, 81.79, 98.14, 104.39, 118.18, 126.22, 151.82, 155.85, 157.04, 158.94, 159.20, 162.10. HRMS (ESI) calcd for $C_{19}H_{26}NaN_4O_4^+$ [M + Na]$^+$ m/z 397.1846 and $C_{38}H_{52}N_8NaO_8$ [2M + Na]$^+$,found m/z 397.1844 and 771.3760.

https://doi.org/10.1021/acs.jmedchem.0c02169
J. Med. Chem. 2021, 64, 8161−8178

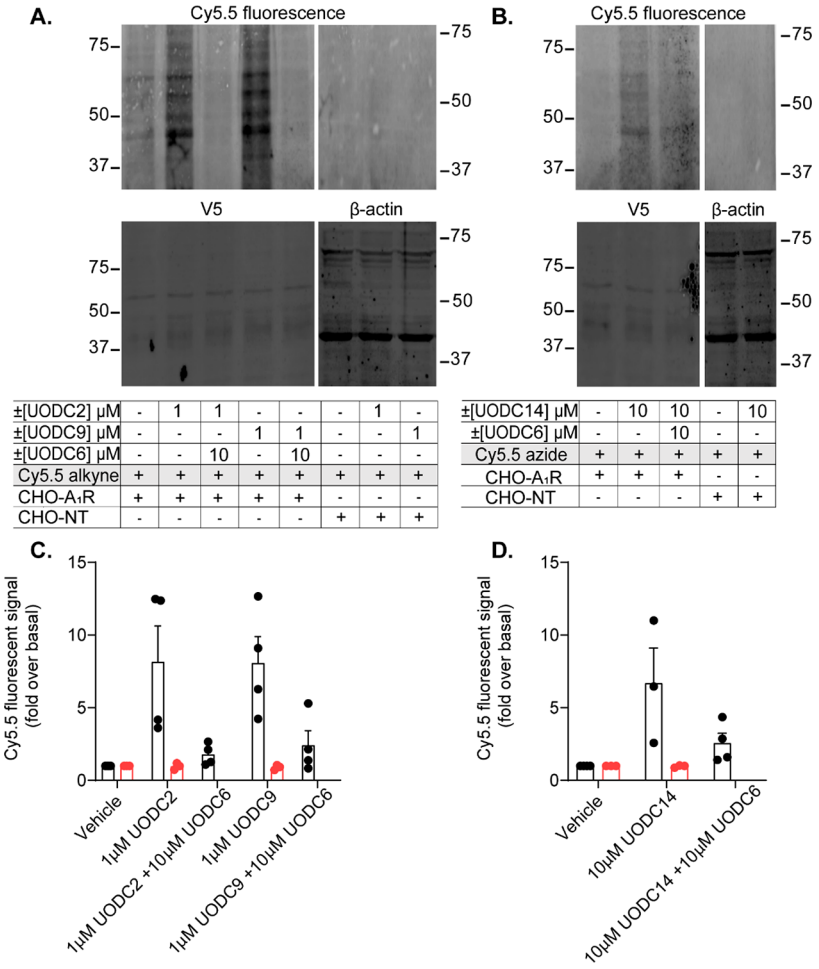

Figure 8. Incorporation of Cy5.5 by **UODC2**, **UODC9**, and **UODC14** is inhibited by preincubation with **UODC6** in hA_1R-FlpIn CHO cells. (A and B) Representative in-gel Cy5.5 fluorescence images coupled with immunoblots for V5 (for hA_1R-FlpInCHO cells) or β-actin (for NT-FlpInCHO cells) shown in gray scale. (C and D) Quantification of fluorescence intensity (prominent bands at 37−50 kDa) labeled by **UODC2**, **UODC9**, and **UODC14** in the absence and presence of an irreversible competitor in hA_1R-FlpInCHO (black) and NT-FlpInCHO (red) cells. Cy5.5 fluorescence was corrected for relative V5 level (for hA_1R-FlpInCHO) or β-actin level (for NT-FlpInCHO). Individual data points are shown with bars to represent means ± SEM from three or four independent experiments.

General Procedure for the Synthesis of 7 and 8. To a stirred suspension of formamidine-protected uracil in methanol was added 2 M aqueous KOH. The suspension was stirred at 50 °C for 1 h. The reaction mixture was cooled to rt and neutralized to pH 7 with 2 M aqueous HCl. After the mixture had been cooled to 5 °C and stirred for 2 h, a precipitate formed, which was collected by filtration, washed with water, and air-dried.

*6-Amino-3-butyl-1-[(2,4-dimethylphenyl)methyl]-1,2,3,4-tetrahydropyrimidine-2,4-dione (**7**).* **5** (3.48 g, 8.95 mmol), methanol (46 mL), and 2 M aqueous KOH (30 mL) gave **7** (2.58 g, 7.73 mmol, 86%) as colorless fluffy crystals. ^{1}H NMR (400 MHz, DMSO-d_6): δ 0.86 (t, J = 7.2 Hz, 3H), 1.23 (m, 2H), 1.43 (m, 2H), 3.71 (t, J = 7.6 Hz, 2H), 3.73 (s, 3H), 3.82 (s, 3H), 4.72 (s, 1H), 4.90 (br s, 2H), 6.49 (dd, J = 2.4, 8.4 Hz), 6.59 (d, J = 2.0 Hz), 6.67 (br s, 2H), 6.71 (d, J = 8.4 Hz). ^{13}C NMR (400 MHz, DMSO-d_6): δ 13.73, 19.61, 29.73, 39.31, 39.94, 55.25, 55.48, 75.16, 98.44, 104.69, 116.25, 126.09, 151.33, 154.56, 157.20, 159.80, 161.20. HRMS (ESI) calcd for $C_{17}H_{24}N_3O_4^+$ $[M + H]^+$ m/z 334.1761 and $C_{17}H_{23}N_3NaO_4^+$ $[M + Na]^+$ m/z 356.1581, found m/z 334.1746 and 356.1559.

*6-Amino-1-[(2,4-dimethylphenyl)methyl]-3-propyl-1,2,3,4-tetrahydropyrimidine-2,4-dione (**8**).* **6** (0.92 g, 2.37 mmol), methanol (7.5 mL), and 2 M aqueous KOH (7.4 mL) gave **8** (0.66 g, 1.98 mmol, 84%) as colorless fluffy crystals. ^{1}H NMR (400 MHz, DMSO-d_6): δ 0.80 (t, J = 7.4 Hz, 3H), 1.47 (m, 2H), 3.67 (t, J = 7.4 Hz, 2H), 3.73 (s, 3H), 3.82 (s, 3H), 4.72 (s, 1H), 4.90 (br s, 2H), 6.49 (dd, J = 2.4, 8.4 Hz), 6.59 (d, J = 2.0 Hz), 6.67 (br s, 2H), 6.71 (d, J = 8.4 Hz). ^{13}C NMR (400 MHz, DMSO-d_6): δ 11.18, 20.87, 40.26, 41.38, 55.26, 55.49, 75.13, 98.45, 104.67, 116.24, 126.05, 151.37, 154.59, 157.21, 159.81, 161.23. HRMS (ESI) calcd for $C_{16}H_{21}N_3NaO_4^+$ $[M + Na]^+$ m/z 342.1424 and $C_{32}H_{42}N_6NaO_8^+$ $[2M + Na]^+$ m/z 661.2956, found m/z 342.1413 and 661.2925.

General Procedure for the Synthesis of 9 and 10. The aminouracil was dissolved in 50% aqueous acetic acid and heated to 70 °C. $NaNO_2$ was added in three batches over 30 min, and the reaction mixture was stirred for 1 h at 70 °C. The mixture was cooled to rt, and the precipitate that formed was collected by filtration, washed with water and diethyl ether, and air-dried to give the nitro intermediate as a pink solid. The solid was dissolved in 25% aqueous ammonia and methanol and heated to 80 °C. $Na_2S_2O_4$ was added in three batches over 30 min, and the reaction mixture was stirred for 4 h at 80 °C. The mixture was cooled to rt and stirred overnight. The crystals that formed were collected by filtration, washed with water and diethyl ether, and air-dried. The product was used in the next reaction immediately without further purification due to instability.

*5,6-Diamino-3-butyl-1-[(2,4-dimethylphenyl)methyl]-1,2,3,4-tetrahydropyrimidine-2,4-dione (**9**).* **7** (2.33 g, 6.98 mmol), 50% aqueous acetic acid (50 mL), and $NaNO_2$ (0.97 g, 14.05 mmol) gave a pink solid (2.33 g). Some of this nitro intermediate (0.70 g), 25% aqueous ammonia (10 mL), methanol (10 mL), and $Na_2S_2O_4$ (0.91 g, 5.22 mmol) gave **9** (0.56 g, 1.59 mmol, 76%) as gray-green crystals. ^{1}H NMR

https://doi.org/10.1021/acs.jmedchem.0c02169
J. Med. Chem. 2021, 64, 8161−8178

(400 MHz, DMSO-d_6): δ 0.87 (t, J = 7.4 Hz, 3H), 1.24 (m, 2H), 1.47 (m, 2H), 3.73 (s, 3H), 3.78 (t, J = 7.2 Hz, 2H), 3.83 (s, 3H), 4.96 (s, 2H), 6.47 (dd, J = 2.4, 8.4 Hz, 1H), 6.59 (d, J = 2.4 Hz, 1H), 6.73 (d, J = 8.4 Hz, 1H). ^{13}C NMR (400 MHz, DMSO-d_6): δ 13.74, 19.61, 29.73, 40.17, 40.33, 55.00, 55.20, 55.25, 96.13, 109.55, 116.53, 126.55, 144.28, 149.60, 157.20, 158.84, 159.82. HRMS (ESI) calcd for $C_{17}H_{24}N_4NaO_4^+$ [M + H]$^+$ m/z 371.1690 and $C_{34}H_{48}N_8NaO_8^+$ [2M + Na]$^+$ m/z 719.3487, found m/z 371.1701 and 719.3495.

*5,6-Diamino-1-[(2,4-dimethylphenyl)methyl]-3-propyl-1,2,3,4-tetrahydropyrimidine-2,4-dione (**10**).* **8** (0.65 g, 2.03 mmol), 50% aqueous acetic acid (15 mL), and $NaNO_2$ (0.28 g, 4.06 mmol) gave a pink solid (0.59 g). This nitro intermediate (0.59 g), 25% aqueous ammonia (8.4 mL), methanol (8.4 mL), and $Na_2S_2O_4$ (0.79 g, 4.54 mmol) gave **10** (0.42 g, 1.26 mmol, 62%) as gray-green crystals.

General Procedure for the Synthesis of Carboxylic Acids 11 and 12. To a suspension of bicyclo[2.2.2]octane-1,4-dicarboxylic acid monomethyl ester in acetonitrile was added Et_3N, and the reaction mixture was stirred for 5 min. HATU was added, and the reaction mixture stirred for 15 min. The diaminouracil, dissolved in acetonitrile, was added dropwise, and the reaction mixture stirred for 1 h. The mixture was concentrated *in vacuo*, and 10% citric acid was added. The aqueous solution was extracted three times with ethyl acetate, and then the pooled organic layers were washed with saturated $NaHCO_3$ and brine and concentrated *in vacuo*. Isopropanol and 1 M aqueous KOH were added, and the reaction mixture was heated at reflux for 1 h. The mixture was cooled and concentrated *in vacuo*; water was added, and the mixture was washed twice with CH_2Cl_2, discarding the organic washings. The aqueous solution was acidified to pH 5 with 12 M aqueous HCl. The mixture was refrigerated overnight, and the resultant precipitate was collected by filtration, rinsed with water, and oven-dried at 80 °C.

*4-{1-Butyl-3-[(2,4-dimethylphenyl)methyl]-2,6-dioxo-2,3,6,9-tetrahydro-1H-purin-8-yl}bicyclo[2.2.2]octane-1-carboxylic Acid (**11**).* Bicyclo[2.2.2]octane-1,4-dicarboxylic acid monomethyl ester (49 mg, 0.23 mmol), acetonitrile (1.0 mL), Et_3N (90 mg, 124 μL, 0.89 mmol), and HATU (88 mg, 0.23 mmol) and then **9** (81 mg, 0.23 mmol), isopropanol (1.10 mL), and 1 M aqueous KOH (1.10 mL) gave **11** (87 mg, 0.17 mmol, 73%) as a white solid. ^{1}H NMR (400 MHz, DMSO-d_6): δ 0.88 (t, J = 7.2 Hz, 3H), 1.27 (m, 2H), 1.50 (m, 2H), 1.70−1.88 (m, 12H), 3.71 (s, 3H), 3.81 (s, 3H), 3.86 (t, J = 7.2 Hz, 2H), 5.04 (s, 2H), 6.39 (dd, J = 2.4, 8.4 Hz, 1H), 6.57 (d, J = 2.4 Hz, 1H), 6.69 (d, J = 8.4 Hz, 1H), 12.07 (br s, 1H), 12.96 (s, 1H). ^{13}C NMR (400 MHz, DMSO-d_6): δ 13.72, 19.61, 27.44, 27.62, 29.38, 29.68, 33.19, 37.63, 37.72, 40.03, 40.27, 40.82, 55.18, 55.49, 98.31, 104.45, 106.49, 116.68, 126.94, 147.55, 150.60, 153.96, 157.42, 159.63, 160.22, 178.41, 178.45. HRMS (ESI) calcd for $C_{27}H_{35}N_4O_6^+$ [M + H]$^+$ m/z 511.2551 and $C_{27}H_{34}N_4NaO_6^+$ [M + Na]$^+$ m/z 533.2371, found m/z 511.2564 and 533.2385.

*4-{3-[(2,4-Dimethoxyphenyl)methyl]-2,6-dioxo-1-propyl-2,3,6,7-tetrahydro-1H-purin-8-yl}bicyclo[2.2.2]octane-1-carboxylic Acid (**12**).* Bicyclo[2.2.2]octane-1,4-dicarboxylic acid monomethyl ester (0.30 g, 1.41 mmol), acetonitrile (5.5 mL), Et_3N (0.55 g, 0.76 mL, 5.43 mmol), and HATU (0.54 g, 1.41 mmol) and then **10** (0.47 g, 1.41 mmol), isopropanol (6 mL), and 1 M aqueous KOH (6 mL) gave **12** (0.42 g, 0.85 mmol, 59%) as a white solid. ^{1}H NMR (400 MHz, DMSO-d_6): δ 0.85 (t, J = 7.4 Hz, 3H), 1.54 (m, 2H), 1.68−1.88 (m, 12H), 3.71 (s, 3H), 3.81 (s, 3H), 3.83 (t, J = 7.2 Hz, 2H), 5.04 (s, 2H), 6.39 (dd, J = 2.4, 8.4 Hz, 1H), 6.57 (d, J = 2.4 Hz, 1H), 6.69 (d, J = 8.4 Hz, 1H), 12.10 (br s, 1H), 12.98 (s, 1H). ^{13}C NMR (400 MHz, DMSO-d_6): δ 11.15, 20.84, 27.62, 29.38, 29.68, 33.18, 37.63, 37.72, 41.07, 42.05, 55.17, 55.49, 98.31, 104.44, 106.49, 116.67, 126.93, 147.55, 150.62, 153.99, 157.41, 159.63, 160.23, 178.40. HRMS (ESI) calcd for $C_{26}H_{31}N_4O_6^-$ [M − H]$^-$ m/z 495.2249, found m/z 495.2242.

*Methyl 4-{1-Butyl-3-[(2,4-dimethoxyphenyl)methyl]-2,6-dioxo-2,3,6,7-tetrahydro-1H-purin-8-yl}bicyclo[2.2.2]octane-1-carboxylate (**13**).* **11** (400 mg, 0.78 mmol) dissolved in methanol (20 mL) and H_2SO_4 (5 drops) were added, and the reaction mixture was stirred at reflux for 3 h. The mixture was cooled to rt overnight, and the resultant crystals were collected by filtration, washed with water, and oven-dried at 80 °C to give **13** (291 mg, 0.55 mmol, 71%) as white fluffy crystals. ^{1}H NMR (400 MHz, DMSO-d_6): δ 0.88 (t, J = 7.4 Hz, 3H), 1.27 (m, 2H), 1.50 (m, 2H), 1.70−1.89 (m, 12H), 3.58 (s, 3H), 3.71 (s, 3H), 3.81 (s, 3H), 3.86 (t, J = 7.4 Hz, 2H), 5.04 (s, 2H), 6.39 (dd, J = 2.4, 8.4 Hz, 1H), 6.57 (d, J = 2.4 Hz, 1H), 6.69 (d, J = 8.4 Hz, 1H), 13.00 (br s, 1H). ^{13}C NMR (400 MHz, DMSO-d_6): δ 13.71, 19.60, 27.58, 29.24, 29.68, 33.11, 38.16, 40.27, 41.07, 51.56, 55.17, 55.48, 98.30, 104.42, 106.52, 116.67, 126.90, 147.54, 150.58, 153.97, 157.40, 159.63, 160.04, 176.97. HRMS (ESI) calcd for $C_{28}H_{36}N_4NaO_6^+$ [M + Na]$^+$ m/z 547.2527, found m/z 547.2509.

General Procedure for the Synthesis of Carboxamides 14–21. The carboxylic acid (**11** or **12**) was dissolved in DMF; then *N*,*N*-diisopropylethylamine (DIPEA) was added, and the reaction mixture stirred for 5 min. HATU was added, and the reaction mixture stirred for 15 min. The NH_2- "linker" (see the Supporting Information) was added dropwise, and the reaction mixture stirred for 2.5 h. The mixture was concentrated *in vacuo*, and then ethyl acetate and saturated aqueous $NaHCO_3$ were added. The aqueous layer was washed twice with ethyl acetate, and the pooled organic phases were concentrated *in vacuo*. The residue was purified using flash column chromatography on silica gel.

*4-{1-Butyl-3-[(2,4-dimethoxyphenyl)methyl]-2,6-dioxo-2,3,6,7-tetrahydro-1H-purin-8-yl}-N-(prop-2-yn-1-yl)bicyclo[2.2.2]octane-1-carboxamide (**14**).* **11** (990 mg, 1.93 mmol), DMF (4 mL), DIPEA (751 mg, 5.81 mmol), HATU (737 mg, 1.93 mmol), and propargyl amine (138 mg, 2.50 mmol) following column elution with *n*-hexane/ethyl acetate (6:4) gave **14** (807 mg, 1.47 mmol, 76%) as a colorless oil. ^{1}H NMR (400 MHz, DMSO-d_6): δ 0.88 (t, J = 7.4 Hz, 3H), 1.27 (m, 2H), 1.50 (m, 2H), 1.66−1.87 (m, 12H), 3.02 (t, J = 2.4 Hz), 3.71 (s, 3H), 3.80 (m, 2H), 3.81 (s, 3H), 3.86 (t, J = 7.4 Hz, 2H), 5.03 (s, 2H), 6.39 (dd, J = 2.4, 8.4 Hz, 1H), 6.57 (d, J = 2.4 Hz, 1H), 6.68 (d, J = 8.4 Hz, 1H), 7.89 (t, J = 5.6 Hz, 1H), 13.00 (br s, 1H). ^{13}C NMR (400 MHz, DMSO-d_6): δ 13.76, 19.65, 27.70, 28.10, 29.59, 29.71, 33.23, 38.13, 38.08, 40.30, 41.13, 55.20, 55.51, 59.80, 72.32, 72.36, 81.79, 98.32, 104.43, 106.55, 116.68, 126.91, 150.61, 154.01, 157.42, 159.66, 176.20, 176.31. HRMS (ESI) calcd for $C_{30}H_{37}N_5NaO5^+$ [M + Na]$^+$ m/z 570.2687 and $C_{60}H_{74}N_{10}NaO_{10}^+$ [2M + Na]$^+$ m/z 1117.5482, found m/z 570.2598 and 1117.5312.

*N-(3-Azidopropyl)-4-{1-butyl-3-[(2,4-dimethoxyphenyl)methyl]-2,6-dioxo-2,3,6,7-tetrahydro-1H-purin-8-yl}bicyclo[2.2.2]octane-1-carboxamide (**15**).* **11** (1.00 g, 1.95 mmol), DMF (4 mL), DIPEA (744 mg, 5.75 mmol), HATU (744 mg, 1.95 mmol), and 3-azidopropan-1-amine (255 mg, 2.54 mmol) following column elution with CH_2Cl_2/methanol (9.7:0.3) gave **15** (985 mg, 1.66 mmol, 85%) as a colorless gummy liquid. ^{1}H NMR (400 MHz, DMSO-d_6): δ 0.88 (t, J = 7.4 Hz, 3H), 1.28 (m, 2H), 1.51 (m, 2H), 1.64 (m, 2H), 1.66−1.87 (m, 12H), 3.09 (q, J = 6.4 Hz, 2H), 3.30 (t, J = 6.8 Hz, 2H), 3.72 (s, 3H), 3.81 (s, 3H), 3.86 (t, J = 7.4 Hz, 2H), 5.04 (s, 2H), 6.39 (dd, J = 2.4, 8.4 Hz, 1H), 6.57 (d, J = 2.4 Hz, 1H), 6.70 (d, J = 8.4 Hz, 1H), 7.47 (t, J = 5.8 Hz, 1H), 12.87 (br s, 1H). ^{13}C NMR (400 MHz, DMSO-d_6): δ 13.70, 19.60, 27.82, 28.39, 29.63, 29.68, 33.21, 36.05, 38.08, 38.23, 40.26, 41.06, 48.47, 55.16, 55.48, 98.31, 104.43, 106.49, 116.71, 126.94, 147.54, 150.58, 153.96, 157.42, 159.64, 160.35, 176.46. HRMS (ESI) calcd for $C_{30}H_{41}N_8O_5^+$ [M + H]$^+$ m/z 593.3194 and $C_{30}H_{40}N_8NaO_5^+$ [M + Na]$^+$ m/z 615.3014, found m/z 593.3187 and 615.3014.

*4-{1-Butyl-3-[(2,4-dimethoxyphenyl)methyl]-2,6-dioxo-2,3,6,9-tetrahydro-1H-purin-8-yl}-N-(hex-5-yn-1-yl)bicyclo[2.2.2]octane-1-carboxamide (**16**).* **11** (100 mg, 0.19 mmol), DMF (1 mL), DIPEA (76 mg, 0.59 mmol), HATU (75 mg, 0.19 mmol), and 5-hexyn-1-amine (28 mg, 0.19 mmol) following column elution with 100% ethyl acetate gave **16** (58 mg, 0.09 mmol, 50%) as a colorless gummy liquid. ^{1}H NMR (400 MHz, DMSO-d_6): δ 0.88 (t, J = 7.4 Hz, 3H), 1.21−1.56 (m, 8H), 1.66−1.87 (m, 12H), 2.14 (t, J = 6.8 Hz, 2H), 2.74 (t, J = 2.8 Hz, 1 H), 3.03 (q, J = 6.3 Hz, 2H), 3.71 (s, 3H), 3.81 (s, 3H), 3.863 (t, J = 7.4 Hz, 2H), 5.04 (s, 2H), 6.39 (dd, J = 2.4, 8.4 Hz, 1H), 6.57 (d, J = 2.4 Hz, 1H), 6.70 (d, J = 8.4 Hz, 1H), 7.40 (t, J = 5.8 Hz, 1H), 12.98 (s, 1H). ^{13}C NMR (400 MHz, DMSO-d_6): δ 13.72, 17.40, 19.61, 25.34, 27.86, 28.26, 29.66, 33.23, 37.94, 38.06, 40.27, 41.07, 55.18, 55.49, 71.22, 84.47, 98.32, 104.45, 106.48, 116.70, 126.94, 147.55, 150.59, 153.96, 157.42, 159.64, 160.39, 162.29, 176.23. HRMS (ESI) calcd for $C_{33}H_{44}N_5O_5^+$ [M + H]$^+$ m/z 590.3337, $C_{33}H_{43}NaN_5O_5^+$ [M + Na]$^+$

https://doi.org/10.1021/acs.jmedchem.0c02169
J. Med. Chem. 2021, 64, 8161−8178

m/z 612.3156, and $C_{66}H_{86}NaN_{10}O_{10}^+$ [2M + Na]$^+$ m/z 1201.6421, found m/z 590.3348, 612.3169, and 1201.6451.

*N-(3-Azidopropyl)-4-{1-butyl-3-[(2,4-dimethoxyphenyl)methyl]-2,6-dioxo-2,3,6,9-tetrahydro-1H-purin-8-yl}bicyclo[2.2.2]octane-1-carboxamide (**17**).* **12** (100 mg, 0.19 mmol), DMF (1 mL), DIPEA (76 mg, 0.59 mmol), HATU (75 mg, 0.19 mmol), and 3-azidopropan-1-amine (20 mg, 0.19 mmol) following column elution with 100% ethyl acetate gave **17** (82 mg, 0.14 mmol, 70%) as a yellowish gummy liquid. ^{1}H NMR (400 MHz, DMSO-d_6): δ 0.85 (t, J = 7.4 Hz, 3H), 1.55 (m, 2H), 1.64 (m, 2H), 1.67−1.88 (m, 12H), 3.09 (q, J = 6.2 Hz, 2H), 3.30 (t, J = 6.8 Hz, 2H), 3.72 (s, 3H), 3.81 (s, 3H), 3.83 (t, J = 7.2 Hz, 2H), 5.04 (s, 2H), 6.39 (dd, J = 2.4, 8.4 Hz, 1H), 6.57 (d, J = 2.4 Hz, 1H), 6.70 (d, J = 8.4 Hz, 1H), 7.47 (t, J = 5.8 Hz, 1H), 12.98 (s, 1H). ^{13}C NMR (400 MHz, DMSO-d_6): δ 11.14, 20.84, 27.81, 28.38, 29.63, 30.76, 33.21, 35.77, 36.05, 38.08, 38.23, 41.06, 42.04, 48.46, 55.17, 55.49, 98.32, 104.45, 106.48, 116.69, 126.93, 147.55, 150.62, 153.98, 157.41, 159.63, 160.36, 162.28, 176.45.

*N-(4-Azidobutyl)-4-{1-butyl-3-[(2,4-dimethoxyphenyl)methyl]-2,6-dioxo-2,3,6,9-tetrahydro-1H-purin-8-yl}bicyclo[2.2.2]octane-1-carboxamide (**18**).* **11** (100 mg, 0.19 mmol), DMF (1 mL), DIPEA (76 mg, 0.59 mmol), HATU (75 mg, 0.19 mmol), and 4-azidobutan-1-amine (22 mg, 0.19 mmol) following column elution with 100% ethyl acetate gave **18** (118 mg, 0.19 mmol, 98%) as a colorless gummy liquid. ^{1}H NMR (400 MHz, DMSO-d_6): δ 0.88 (t, J = 7.4 Hz, 3H), 1.28 (m, 2H), 1.39−1.55 (m, 6H), 1.66−1.87 (m, 12H), 3.04 (q, J = 6.2 Hz, 2H), 3.31 (t, J = 6.4 Hz, 2H), 3.72 (s, 3H), 3.81 (s, 3H), 3.86 (t, J = 7.4 Hz, 2H), 5.04 (s, 2H), 6.39 (dd, J = 2.4, 8.4 Hz, 1H), 6.57 (d, J = 2.4 Hz, 1H), 6.70 (d, J = 8.4 Hz, 1H), 7.43 (t, J = 5.8 Hz, 1H), 12.97 (s, 1H). ^{13}C NMR (400 MHz, DMSO-d_6): δ 13.71, 19.60, 25.59, 26.32, 27.85, 29.65, 29.68, 30.76, 33.21, 38.06, 38.24, 40.26, 41.06, 50.34, 55.18, 55.49, 98.31, 104.45, 106.50, 116.70, 126.94, 147.55, 150.59, 153.97, 157.42, 159.64, 160.38, 176.29. HRMS (ESI) calcd for $C_{31}H_{42}NaN_8O_5^+$ [M + Na]$^+$ m/z 629.3170, found m/z 629.3133.

*N-(8-Azidooctyl)-4-{1-butyl-3-[(2,4-dimethoxyphenyl)methyl]-2,6-dioxo-2,3,6,9-tetrahydro-1H-purin-8-yl}bicyclo[2.2.2]octane-1-carboxamide (**19**).* **11** (100 mg, 0.19 mmol), DMF (1 mL), DIPEA (76 mg, 0.59 mmol), HATU (75 mg, 0.19 mmol), and 8-azidooctan-1-amine hydrochloride (40 mg, 0.19 mmol) (preneutralized with 1 equiv of DIPEA) following column elution with 100% ethyl acetate gave **19** (100 mg, 0.15 mmol, 77%) as a colorless gummy liquid. ^{1}H NMR (400 MHz, DMSO-d_6): δ 0.88 (t, J = 7.4 Hz, 3H), 1.14−1.41 (m, 12H), 1.45−1.56 (m, 4H), 1.64−1.88 (m, 12H), 3.01 (q, J = 6.6 Hz), 3.30 (t, J = 6.8 Hz, 2H), 3.72 (s, 3H), 3.81 (s, 3H), 3.86 (t, J = 7.4 Hz, 2H), 5.04 (s, 2H), 6.39 (dd, J = 2.4, 8.4 Hz, 1H), 6.57 (d, J = 2.4 Hz, 1H), 6.70 (d, J = 8.4 Hz, 1H), 7.35 (t, J = 5.8 Hz, 1H), 12.97 (s, 1H). ^{13}C NMR (400 MHz, DMSO-d_6): δ 13.71, 19.59, 26.07, 26.17, 27.85, 28.21, 28.46, 28.58, 29.03, 29.66, 33.21, 38.02, 38.52, 39.98, 40.74, 40.25, 41.05, 50.61, 54.90, 55.17, 55.48, 98.31, 104.44, 106.48, 116.69, 126.94, 147.54, 150.58, 153.95, 157.41, 159.63, 160.38, 176.11. HRMS (ESI) calcd for $C_{35}H_{50}NaN_8O_5^+$ [M + Na]$^+$ m/z 685.3796 and $C_{70}H_{100}N_{16}NaO_{16}^+$ [2M + Na]$^+$ m/z 1347.7701, found m/z 685.3792 and 1347.7668.

*N-{2-[2-(2-Azidoethoxy)ethoxy]ethyl}-4-{1-butyl-3-[(2,4-dimethoxyphenyl)methyl]-2,6-dioxo-2,3,6,9-tetrahydro-1H-purin-8-yl}bicyclo[2.2.2]octane-1-carboxamide (**20**).* **11** (200 mg, 0.39 mmol), DMF (1 mL), DIPEA (152 mg, 1.18 mmol), HATU (149 mg, 0.39 mmol), and 2-[2-(2-azidoethoxy)ethoxy]ethan-1-amine (68 mg, 0.39 mmol) following column elution with 100% ethyl acetate gave **20** (190 mg, 0.28 mmol, 72%) as a colorless gummy liquid. ^{1}H NMR (400 MHz, DMSO-d_6): δ 0.88 (t, J = 7.4 Hz, 3H), 1.27 (m, 2H), 1.51 (m, 2H), 1.62−1.90 (m, 12H), 3.18 (q, J = 6 Hz, 2H), 3.36−3.41 (m, 4H), 3.48−3.57 (m, 4H), 3.59 (t, J = 5.0 Hz, 2H), 3.72 (s, 3H), 3.81 (s, 3H), 3.86 (t, J = 7.4 Hz, 2H), 5.04 (s, 2H), 6.39 (dd, J = 2.4, 8.4 Hz, 1H), 6.57 (d, J = 2.4 Hz, 1H), 6.70 (d, J = 8.4 Hz, 1H), 7.39 (t, J = 5.8 Hz, 1H), 12.97 (br s, 1H). ^{13}C NMR (400 MHz, DMSO-d_6): δ 13.71, 19.60, 27.78, 29.62, 29.68, 33.21, 38.07, 38.58, 40.08, 40.26, 41.06, 49.99, 55.18, 55.49, 68.91, 69.24, 69.59, 69.61, 98.31, 104.45, 106.48, 116.69, 126.93, 147.54, 150.59, 153.95, 157.41, 159.63, 160.35, 176.47. HRMS (ESI) calcd for $C_{33}H_{46}N_8NaO_7^+$ [M + Na]$^+$ m/z 689.3382 and $C_{66}H_{92}N_{16}NaO_{14}^+$ [2M + Na]$^+$ m/z 1355.6871, found m/z 689.3332 and 1355.6796.

*N-(2-{2-[2-(2-Azidoethoxy)ethoxy]ethoxy}ethyl)-4-{1-butyl-3-[(2,4-dimethoxyphenyl)methyl]-2,6-dioxo-2,3,6,9-tetrahydro-1H-purin-8-yl}bicyclo[2.2.2]octane-1-carboxamide (**21**).* **11** (200 mg, 0.39 mmol), DMF (1 mL), DIPEA (152 mg, 1.18 mmol), HATU (149 mg, 0.39 mmol), and {2-[2-(2-azidoethoxy)ethoxy]ethoxy}-methanamine (85 mg, 0.39 mmol) following column elution with ethyl acetate/methanol (9.5:0.5) gave **21** (200 mg, 0.29 mmol, 75%) as a colorless gummy liquid. ^{1}H NMR (400 MHz, DMSO-d_6): δ 0.88 (t, J = 7.4 Hz, 3H), 1.27 (m, 2H), 1.50 (m, 2H), 1.64−1.89 (m, 12H), 3.18 (q, J = 6.2 Hz, 2H), 3.38 (t, J = 5.2 Hz, 4H), 3.45−3.57 (m, 8H), 3.59 (t, J = 4.8 Hz, 2H), 5.04 (s, 2H), 6.39 (dd, J = 2.2, 8.6 Hz, 1H), 6.57 (d, J = 2.0 Hz, 1H), 6.69 (d, J = 8.4 Hz, 1H), 7.40 (t, J = 5.6 Hz, 1H), 12.97 (s, 1H). ^{13}C NMR (400 MHz, DMSO-d_6): δ 13.72, 19.60, 27.81, 29.66, 29.70, 33.22, 35.78, 38.08, 38.59, 40.08, 40.83, 49.98, 55.18, 55.49, 68.87, 69.25, 69.57, 69.70, 69.75, 69.79, 98.31, 104.44, 116.73, 126.92, 147.53, 150.61, 153.98, 157.41, 159.62, 162.29, 176.51. HRMS (ESI) calcd for $C_{35}H_{51}N_8O_8^+$ [M + H]$^+$ m/z 711.3824 and $C_{35}H_{50}N_8NaO_8^+$ [M + Na]$^+$ m/z 733.3644, found m/z 711.3839 and 733.3662.

General Procedure for the Synthesis of Sulfonyl Fluorides UODC2, UODC5, UODC6, UODC9−UODC14. The DMB-protected carboxamide was dissolved in neat TFA and stirred overnight at 50 °C. The reaction mixture was cooled to rt and blown with compressed air for 20 min to evaporate excess TFA. CH_2Cl_2 was added, and the organic solution was concentrated *in vacuo* and then dried overnight under high vacuum. The residue was dissolved in DMF, K_2CO_3 added, and the reaction mixture stirred for 45 min. 4-[(3-Bromopropyl)carbamoyl]-benzenesulfonyl fluoride (in a solution of DMF) was added dropwise, and the reaction mixture was stirred overnight. The reaction mixture was concentrated *in vacuo*, and water was added. The aqueous solution was extracted three times with ethyl acetate. The pooled organic layers were dried with $MgSO_4$, filtered, and concentrated *in vacuo*. The crude product was purified by column chromatography and underwent subsequent semipreparative RP-HPLC purification.

*Methyl 4-[1-Butyl-3-(3-{[4-(fluorosulfonyl)phenyl]formamido}-propyl)-2,6-dioxo-2,3,6,9-tetrahydro-1H-purin-8-yl]bicyclo[2.2.2]-octane-1-carboxylate (**UODC6**).* **13** (290 mg, 0.55 mmol), TFA (2 mL), DMF (4 mL), K_2CO_3 (77 mg, 0.55 mmol), and 4-[(3-bromopropyl)carbamoyl]benzenesulfonyl fluoride (270 mg, 0.83 mmol) (in a solution of DMF) following column elution with CH_2Cl_2/$(CH_3)_2CO$ (9:1) gave a white solid (218 mg). Some of this white solid (68 mg) was further purified by semipreparative RP-HPLC to give **UODC6** (15 mg, 0.024 mmol, 15%) as white crystals. ^{1}H NMR (500 MHz, DMSO-d_6): δ 0.88 (t, J = 7.3 Hz, 3H), 1.27 (m, 2H), 1.50 (m, 2H), 1.64−1.81 (m, 12H), 1.96 (m, 2H), 3.31 (q, J = 6.3 Hz, 2H), 3.58 (s, 3H), 3.85 (t, J = 7.3 Hz, 2H), 4.06 (t, J = 7.0 Hz, 2H), 8.17 (d, J = 8.5 Hz, 2H), 8.27 (d, J = 8.5 Hz, 2H), 8.86 (t, J = 5.5 Hz, 1H), 12.96 (br s, 1H). ^{13}C NMR (500 MHz, DMSO-d_6): δ 13.71, 19.62, 27.44, 27.51, 29.16, 29.68, 33.02, 36.85, 38.10, 40.22, 40.43, 40.68, 51.53, 106.51, 128.60, 129.00, 133.41 (d), 141.54, 147.21, 150.59, 153.88, 157.55, 158.00, 159.92, 164.20, 176.89. ^{19}F NMR (400 MHz, DMSO-d_6): δ 66.13. HRMS (ESI) calcd for $C_{29}H_{36}FN_5NaO_7S^+$ [M + Na]$^+$ m/z 640.2212 and $C_{58}H_{72}F_2N_{10}NaO_{14}S_2^+$ [2M + Na]$^+$ m/z 1257.4531, found m/z 640.2177 and 1257.4438. HPLC: 19.28 min.

*4-{[3-(1-Butyl-2,6-dioxo-8-{4-[(prop-2-yn-1-yl)carbamoyl]-bicyclo[2.2.2]octan-1-yl}-2,3,6,9-tetrahydro-1H-purin-3-yl)propyl]-carbamoyl}benzene-1-sulfonyl Fluoride (**UODC5**).* **14** (508 mg, 0.93 mmol), TFA (3 mL), DMF (4 mL), K_2CO_3 (128 mg, 0.93 mmol), and 4-[(3-bromopropyl)carbamoyl]benzenesulfonyl fluoride (270 mg, 0.83 mmol) (in a solution of DMF) following column elution with CH_2Cl_2/$(CH_3)_2CO$ (7:3) gave a white solid (300 mg). Some of this white solid (101 mg) was further purified by semipreparative RP-HPLC to give **UODC5** (16 mg, 0.025 mmol, 12%) as white crystals. ^{1}H NMR (500 MHz, DMSO-d_6): δ 0.88 (t, J = 7.3 Hz, 3H), 1.28 (m, 2H), 1.50 (m, 2H), 1.77−1.88 (m, 12H), 1.97 (m, 2H), 2.24 (s, 1H), 2.24 (s, 2H), 3.31 (q, J = 6.5 Hz, 2H), 3.86 (t, J = 7.3 Hz, 2H), 4.08 (t, J = 7.0 Hz, 2H), 6.66 (m, 1H), 8.17 (d, J = 8.0 Hz, 2H), 8.26 (d, J = 9.0 Hz, 2H), 8.87 (t, J = 5.5 Hz, 1H), 12.98 (br s, 1H). ^{13}C NMR (500 MHz, DMSO-d_6): δ 10.49, 13.70, 19.62, 27.45, 29.05, 29.33, 29.68, 32.86, 33.11,

https://doi.org/10.1021/acs.jmedchem.0c02169
J. Med. Chem. 2021, 64, 8161−8178

36.88, 40.23, 40.69, 106.52, 122.14, 128.60, 129.00, 133.32, 133.51, 141.54, 147.25, 147.74, 150.60, 153.88, 160.04, 164.20, 167.65. ^{19}F NMR (400 MHz, DMSO-d_6): δ 66.19. HRMS (ESI) calcd for $C_{31}H_{37}FN_6NaO_6S^+$ $[M + Na]^+$ m/z 663.2372 and $C_{62}H_{74}F_2N_{12}NaO_{12}S^+$ $[2M + Na]^+$ m/z 1303.4851, found m/z 663.2321 and 1303.4685. HPLC: 19.24 min.

*4-{[3-(8-{4-[(3-Azidopropyl)carbamoyl]bicyclo[2.2.2]octan-1-yl}-1-butyl-2,6-dioxo-2,3,6,9-tetrahydro-1H-purin-3-yl)propyl]-carbamoyl}benzene-1-sulfonyl Fluoride (**UODC2**).* **15** (469 mg, 0.79 mmol), TFA (2.5 mL), DMF (4 mL), K_2CO_3 (109 mg, 0.79 mmol), and 4-[(3-bromopropyl)carbamoyl]benzenesulfonyl fluoride (230 mg, 0.71 mmol) (in a solution of DMF) following column elution with $CH_2Cl_2/(CH_3)_2CO$ (7:3) gave a white solid (190 mg). Some of this white solid (76 mg) was further purified by semipreparative RP-HPLC to give **UODC2** (22 mg, 0.032 mmol, 11%) as white crystals. ^{1}H NMR (500 MHz, DMSO-d_6): δ 0.80 (t, J = 7.3 Hz, 3H), 1.27 (m, 2H), 1.50 (m, 2H), 1.65 (m, 2H), 1.65−1.81 (m, 12H), 1.96 (m, 2H), 3.09 (q, J = 6.3 Hz, 2H), 3.31 (t, J = 6.8 Hz, 2H), 3.31 (q, J = 6.5 Hz, 2H), 3.86 (t, J = 7.5 Hz, 2H), 4.06 (t, J = 7 Hz, 2H), 7.45 (t, J = 5.8 Hz, 1H), 8.16 (d, J = 8.5 Hz, 2H), 8.25 (d, J = 9.0 Hz, 2H), 8.85 (t, J = 5.5 Hz, 1H), 12.94 (s, 1H). ^{13}C NMR (500 MHz, DMSO-d_6): δ 13.71, 19.62, 27.49, 27.77, 28.40, 29.58, 29.68, 33.15, 36.04, 36.95, 38.05, 40.22, 40.73, 48.47, 106.53, 128.59, 128.98, 133.41 (d), 141.54, 147.20, 150.61, 153.88, 157.97, 158.25, 160.25, 164.23, 176.40. ^{19}F NMR (400 MHz, DMSO-d_6): δ 66.18. HRMS (ESI) calcd for $C_{31}H_{40}FN_9NaO_6S^+$ $[M + Na]^+$ m/z 708.2699 and $C_{62}H_{80}F_2N_{18}NaO_{12}S_2^+$ $[2M + Na]^+$ m/z 1393.5505, found m/z 708.2656 and 1393.5440. HPLC: 18.49 min.

*4-{[3-(1-Butyl-8-{4-[(hex-5-yn-1-yl)carbamoyl]bicyclo[2.2.2]-octan-1-yl}-2,6-dioxo-2,3,6,9-tetrahydro-1H-purin-3-yl)propyl]-carbamoyl}benzene-1-sulfonyl Fluoride (**UODC14**).* **16** (100 mg, 0.17 mmol), TFA (1 mL), DMF (2 mL), K_2CO_3 (23 mg, 0.17 mmol), and 4-[(3-bromopropyl)carbamoyl]benzenesulfonyl fluoride (49 mg, 0.15 mmol) (in a solution of DMF) following column elution with 100% ethyl acetate and then semipreparative RP-HPLC purification of all material gave **UODC14** (35 mg, 0.051 mmol, 33%) as white crystals. ^{1}H NMR (400 MHz, DMSO-d_6): δ 0.88 (t, J = 7.4 Hz, 3H), 1.27 (m, 2H), 1.35−1.54 (m, 8H), 1.61−1.83 (m, 12H), 1.96 (m, 2H), 2.15 (t, J = 6.2 Hz, 2H), 2.74 (t, J = 2.4 Hz, 1H), 3.03 (q, J = 6.4 Hz, 2H), 3.31 (q, J = 6.6 Hz, 2H), 3.85 (t, J = 7.5 Hz, 2H), 4.06 (t, J = 7 Hz, 2H), 7.39 (t, J = 5.8 Hz, 1H), 8.15 (d, J = 8.4 Hz, 2H), 8.25 (d, J = 8.5 Hz, 2H), 8.85 (t, J = 5.6 Hz, 1H), 12.94 (s, 1H). ^{13}C NMR (400 MHz, DMSO-d_6): δ 13.73, 17.41, 19.64, 25.34, 27.51, 27.82, 27.96, 28.27, 29.62, 29.69, 36.48, 37.95, 38.04, 40.24, 40.74, 71.22, 84.47, 106.51, 128.61, 128.99, 133.41 (d), 141.54, 147.23, 150.62, 153.88, 160.33, 160.91, 164.23, 176.18. ^{19}F NMR (400 MHz, DMSO-d_6): δ −69.31, −71.20 (TFA salt), 66.13. HRMS (ESI) calcd for $C_{34}H_{44}FN_6O_6S^+$ $[M + H]^+$ m/z 683.3022 and $C_{34}H_{43}FNaN_6O_6S^+$ $[M + Na]^+$ m/z 705.2841, found m/z 683.3035 and 705.2856. HPLC: 19.39 min.

*4-{[3-(8-{4-[(3-Azidopropyl)carbamoyl]bicyclo[2.2.2]octan-1-yl}-2,6-dioxo-1-propyl-2,3,6,9-tetrahydro-1H-purin-3-yl)propyl]-carbamoyl}benzene-1-sulfonyl Fluoride (**UODC9**).* **17** (50 mg, 0.08 mmol), TFA (1 mL), DMF (2 mL), K_2CO_3 (12 mg, 0.08 mmol), and 4-[(3-bromopropyl)carbamoyl]benzenesulfonyl fluoride (25 mg, 0.07 mmol) (in a solution of DMF) following column elution with 100% ethyl acetate gave a white solid (107 mg). Some of this solid (39 mg) was further purified by semipreparative RP-HPLC to give **UODC9** (11 mg, 0.016 mmol, 71%) as white crystals. ^{1}H NMR (500 MHz, DMSO-d_6): δ 0.85 (t, J = 7.3 Hz, 3H), 1.54 (m, 2H), 1.65 (m, 2H), 1.62−1.81 (m, 12H), 1.96 (m, 2H), 3.09 (q, J = 6.3 Hz, 2H), 3.31 (t, J = 6.8 Hz, 2H), 3.82 (t, J = 7.5 Hz, 2H), 4.06 (t, J = 7.0 Hz, 2H), 7.45 (t, J = 5.8 Hz, 2H), 8.16 (d, J = 8.0 Hz, 1H), 8.26 (d, J = 8.5 Hz, 1H), 8.86 (t, J = 5.5 Hz, 1H), 12.94 (s, 1H). ^{13}C NMR (500 MHz, DMSO-d_6): δ 11.20, 20.86, 27.51, 27.79, 28.41, 29.60, 33.18, 36.08, 36.97, 38.07, 40.75, 42.04, 48.49, 106.54, 128.63, 129.02, 133.43 (d), 141.57, 147.24, 150.68, 153.94, 157.89, 158.14, 160.32, 164.30, 176.47. ^{19}F NMR (400 MHz, DMSO-d_6): δ 66.15. HRMS (ESI) calcd for $C_{30}H_{38}FNaN_9O_6S^+$ $[M + Na]^+$ m/z 694.2542, found m/z 694.2537. HPLC: 18.17 min.

*4-{[3-(8-{4-[(4-Azidobutyl)carbamoyl]bicyclo[2.2.2]octan-1-yl}-1-butyl-2,6-dioxo-2,3,6,9-tetrahydro-1H-purin-3-yl)propyl]-carbamoyl}benzene-1-sulfonyl Fluoride (**UODC10**).* **18** (100 mg, 0.16 mmol), TFA (1 mL), DMF (2 mL), K_2CO_3 (22 mg, 0.16 mmol), and 4-[(3-bromopropyl)carbamoyl]benzenesulfonyl fluoride (48 mg, 0.15 mmol) (in a solution of DMF) following column elution with 100% ethyl acetate and then semipreparative RP-HPLC purification gave **UODC10** (20 mg, 0.02 mmol, 19%) as white crystals. ^{1}H NMR (500 MHz, DMSO-d_6): δ 0.88 (t, J = 7.3 Hz, 3H), 1.27 (m, 2H), 1.40−1.55 (m, 6H), 1.60−1.84 (m, 12H), 1.96 (m, 2H), 3.05 (q, J = 6.2 Hz, 2H), 3.34 (q, J = overlap, 2H), 3.34 (t, J = overlap), 3.86 (t, J = 7.3 Hz, 2H), 4.06 (t, J = 7.0 Hz, 2H), 7.40 (t, J = 5.8 Hz, 1H), 8.16 (d, J = 8.5 Hz, 1H), 8.26 (d, J = 8.5 Hz, 1H), 8.86 (t, J = 5.8 Hz, 1H), 12.94 (s, 1H). ^{19}F NMR (400 MHz, DMSO-d_6): δ −73.72 (TFA salt), 66.15. HRMS (ESI) calcd for $C_{32}H_{42}FNaN_9O_6S^+$ $[M + Na]^+$ m/z 722.2855, found m/z 722.2849. HPLC: 19.31 min.

*4-{[3-(8-{4-[(8-Azidooctyl)carbamoyl]bicyclo[2.2.2]octan-1-yl}-1-butyl-2,6-dioxo-2,3,6,9-tetrahydro-1H-purin-3-yl)propyl]-carbamoyl}benzene-1-sulfonyl Fluoride (**UODC11**).* **19** (80 mg, 0.12 mmol), TFA (1 mL), DMF (2 mL), K_2CO_3 (17 mg, 0.12 mmol), and 4-[(3-bromopropyl)carbamoyl]benzenesulfonyl fluoride (35 mg, 0.11 mmol) (in a solution of DMF) following column elution with 100% ethyl acetate and then semipreparative RP-HPLC purification gave **UODC11** (30 mg, 0.039 mmol, 36%) as white crystals. ^{1}H NMR (500 MHz, DMSO-d_6): δ 0.88 (t, J = 7.3 Hz, 3H), 1.16−1.41 (m, 12H), 1.46−1.56 (m, 4H), 1.61−1.81 (m, 12H), 1.96 (m, 2H), 3.00 (q, J = 6.5 Hz, 2H), 3.31 (q, J = overlap, 2H), 3.31 (t, J = overlap, 2H), 3.85 (t, J = 7.5 Hz, 2H), 4.06 (t, J = 7.0 Hz, 2H), 7.32 (t, J = 5.8 Hz, 1H), 8.15 (d, J = 8.5 Hz, 1H), 8.25 (d, J = 8.5 Hz, 1H), 8.85 (t, J = 5.8 Hz, 1H), 12.93 (s, 1H). ^{13}C NMR (500 MHz, DMSO-d_6): δ 13.75, 19.64, 26.11, 26.20, 27.49, 27.82, 28.24, 28.48, 28.63, 29.07, 29.63, 29.71, 30.71, 33.18, 36.97, 38.02, 38.56, 40.25, 40.75, 50.65, 106.52, 128.62, 129.01, 133.41 (d), 141.57, 147.25, 150.64, 153.90, 157.60, 157.85, 158.10, 160.34, 164.28, 176.12. ^{19}F NMR (400 MHz, DMSO-d_6): δ −73.75 (TFA salt), 66.18. HRMS (ESI) calcd for $C_{36}H_{51}FN_9O_6S^+$ $[M + H]^+$ m/z 756.3662 and $C_{36}H_{50}FNaN_9O_6S^+$ $[M + Na]^+$ m/z 778.3481, found m/z 756.3661 and 778.3473. HPLC: 21.75 min.

*4-[(3-{8-[4-({2-[2-(2-Azidoethoxy)ethoxy]ethyl}carbamoyl)-bicyclo[2.2.2]octan-1-yl]-1-butyl-2,6-dioxo-2,3,6,9-tetrahydro-1H-purin-3-yl}propyl)carbamoyl]benzene-1-sulfonyl Fluoride (**UODC12**).* **20** (43 mg, 0.06 mmol), TFA (1 mL), DMF (2 mL), K_2CO_3 (9 mg, 0.06 mmol), and 4-[(3-bromopropyl)carbamoyl]-benzenesulfonyl fluoride (19 mg, 0.05 mmol) (in a solution of DMF) following column elution with 100% ethyl acetate and then semi-preparative RP-HPLC purification gave **UODC12** (19 mg, 0.02 mmol, 43%) as white crystals. ^{1}H NMR (500 MHz, DMSO-d_6): δ 0.88 (t, J = 7.5 Hz, 3H), 1.27 (m, 2H), 1.50 (m, 2H), 1.62−1.82 (m, 12H), 1.96 (m, 2H), 3.18 (q, J = 6 Hz, 2H), 3.31 (q, J = 6.5 Hz, 2H), 3.35−3.62 (m, 8H), 3.60 (t, J = 4.8 Hz, 2H), 3.85 (t, J = 7.5 Hz, 2H), 4.06 (t, J = 7 Hz, 2H), 7.36 (t, J = 5.8 Hz, 1H), 8.15 (d, J = 8.5 Hz, 2H), 8.25 (d, J = 8.5 Hz, 2H), 8.85 (t, J = 5.8 Hz, 1H), 12.93 (s, 1H). ^{13}C NMR (500 MHz, DMSO-d_6): δ 13.74, 19.64, 27.52, 27.76, 29.59, 29.71, 30.71, 33.18, 37.00, 38.07, 38.60, 40.26, 40.77, 50.03, 68.94, 69.27, 69.64, 106.54, 106.91, 128.62, 129.01, 133.42 (d), 141.57, 147.24, 150.64, 153.64, 157.91, 158.17, 160.30, 164.28, 176.48. ^{19}F NMR (400 MHz, DMSO-d_6): δ −74.41 (TFA salt), 66.18. HRMS (ESI) calcd for $C_{34}H_{47}FN_9O_8S^+$ $[M + H]^+$ m/z 760.3247 and $C_{34}H_{46}FNaN_9O_8S^+$ $[M + Na]^+$ m/z 782.3066, found m/z 760.3246 and 782.3062. HPLC: 18.91 min.

*4-{[3-(8-{4-[(2-{2-[2-(2-Azidoethoxy)ethoxy]ethoxy}ethyl)-carbamoyl]bicyclo[2.2.2]-octan-1-yl}-1-butyl-2,6-dioxo-2,3,6,9-tetrahydro-1H-purin-3-yl)propyl]carbamoyl}-benzene-1-sulfonyl Fluoride (**UODC13**).* **21** (69 mg, 0.09 mmol), TFA (1 mL), DMF (2 mL), K_2CO_3 (14 mg, 0.09 mmol), and 4-[(3-bromopropyl)-carbamoyl]benzenesulfonyl fluoride (28 mg, 0.08 mmol) (in a solution of DMF) following column elution with 100% ethyl acetate and then semipreparative RP-HPLC purification gave **UODC13** (19 mg, 0.023 mmol, 27%) as white crystals. ^{1}H NMR (500 MHz, DMSO-d_6): δ 0.88 (t, J = 7.5 Hz, 3H), 1.27 (m, 2H), 1.50 (m, 2H), 1.62−1.83 (m, 12H), 1.96 (m, 2H), 3.18 (q, J = 6 Hz, 2H), 3.31 (q, J = 6.5 Hz, 2H), 3.35−3.62 (m, 12H), 3.60 (t, J = 5.0 Hz, 2H), 3.85 (t, J = 7.5 Hz, 2H), 4.06 (t, J = 7 Hz, 2H), 7.37 (t, J = 5.5 Hz, 1H), 8.15 (d, J = 8.5 Hz, 2H), 8.25 (d, J = 8.5 Hz, 2H), 8.85 (t, J = 5.8 Hz, 1H), 12.93 (s, 1H). ^{13}C NMR (500 MHz, DMSO-d_6): δ 13.72, 19.63, 27.51, 27.75, 29.58, 29.69, 33.16, 36.99, 38.06, 38.60, 40.24, 40.75, 50.00, 68.90, 69.27, 69.60, 69.71,

https://doi.org/10.1021/acs.jmedchem.0c02169
J. Med. Chem. 2021, 64, 8161−8178

69.77, 69.80, 106.53, 128.60, 128.99, 133.41 (d), 141.55, 147.21, 150.62, 153.89, 157.88, 158.14, 160.28, 164.24, 176.44. ^{19}F NMR (400 MHz, DMSO-d_6): δ −74.10 (TFA salt), 66.16. HRMS (ESI) calcd for $C_{36}H_{50}FNaN_9O_9S^+$ $[M + Na]^+$ m/z 826.3328, found m/z 826.3326. HPLC: 19.00 min.

General Procedure for the Synthesis of Sulfonic Acids UODC7 and UODC3. The sulfonyl fluoride was dissolved in 1 M methanolic NaOH and stirred for 1 h. The reaction mixture was acidified to pH 4 with 12 M HCl and concentrated *in vacuo*. Ethyl acetate was added, and then the organic layer was washed with saturated aqueous $NaHCO_3$ and concentrated *in vacuo*.

*4-[(3-{1-Butyl-8-[4-(methoxycarbonyl)bicyclo[2.2.2]octan-1-yl]-2,6-dioxo-2,3,6,9-tetrahydro-1H-purin-3-yl}propyl)carbamoyl]-benzene-1-sulfonic Acid (**UODC7**).* **UODC6** (24 mg, 0.039 mmol) and 1 M methanolic NaOH (2 mL) following semipreparative RP-HPLC purification gave **UODC7** (21 mg, 0.034 mmol, 88%) as a white solid. ^{1}H NMR (500 MHz, DMSO-d_6): δ 0.89 (t, J = 7.3 Hz, 3H), 1.28 (m, 2H), 1.51 (m, 2H), 1.73−1.90 (m, 12H), 1.92 (m, 2H), 3.27 (q, J = 6.8 Hz, 2H), 3.59 (s, 3H), 3.86 (t, J = 7.3 Hz, 2H), 4.04 (t, J = 7 Hz, 2H), 6.54 (br s, 1H), 7.64 (d, J = 8.5 Hz, 2H), 7.75 (d, J = 8 Hz, 2H), 8.44 (t, J = 5.8 Hz, 1H), 12.98 (s, 1H). ^{13}C NMR (500 MHz, DMSO-d_6): δ 13.72, 19.62, 27.58, 27.85, 29.25, 29.68, 33.11, 36.78, 38.17, 40.24, 40.86, 51.57, 106.53, 125.34, 126.63, 134.44, 147.24, 150.61, 150.73, 153.87, 157.64, 157.89, 160.04, 165.79, 176.98. HRMS (ESI) calcd for $C_{29}H_{37}N_5O_8S^-$ $[M - H]^-$ m/z 614.2290, found m/z 614.2249. HPLC: 14.29 min.

*4-{[3-(8-{4-[(3-Azidopropyl)carbamoyl]bicyclo[2.2.2]octan-1-yl}-1-butyl-2,6-dioxo-2,3,6,9-tetrahydro-1H-purin-3-yl)propyl]-carbamoyl}benzene-1-sulfonic Acid (**UODC3**).* **UODC2** (21 mg, 0.031 mmol) and 1 M methanolic NaOH (2 mL) following semipreparative RP-HPLC purification gave **UODC3** (19 mg, 0.028 mmol, 95%) as a white solid. ^{1}H NMR (500 MHz, DMSO-d_6): δ 0.89 (t, J = 7.3 Hz, 3H), 1.28 (m, 2H), 1.51 (m, 2H), 1.57−1.73 (m, 12H), 1.68 (m, 2H), 1.93 (m, 2H), 3.10 (q, J = 6.3 Hz, 2H), 3.26 (q, J = 6.3 Hz, 2H), 3.32 (t, J = 7.0 Hz, 2H), 3.86 (t, J = 7.5 Hz, 2H), 4.06 (t, J = 7.0 Hz, 2H), 4.99 (br s, 1H), 7.51 (t, J = 5.8 Hz, 1H), 7.69 (d, J = 8.5 Hz, 2H), 7.81 (d, J = 8.5 Hz, 2H), 8.46 (t, J = 5.8 Hz, 1H), 12.85 (br s, 1H). ^{13}C NMR (500 MHz, DMSO-d_6): δ 13.74, 19.63, 27.58, 27.76, 28.36, 29.50, 29.70, 33.10, 36.10, 36.26, 38.00, 40.19, 40.68, 40.43, 48.59, 106.42, 125.40, 126.79, 134.67, 147.27, 150.44, 150.61, 153.89, 158.18, 158.48, 160.26, 165.83, 176.43. HRMS (ESI) calcd for $C_{31}H_{40}N_9O_7S^-$ $[M - H]^-$ m/z 682.2777, found m/z 682.2761. HPLC: 14.04 min.

General Procedure for POM Protection to Give 22 and 23. The xanthine was dissolved in DMF, K_2CO_3 added, and the reaction mixture stirred for 45 min at 50 °C. Pivaloxymethyl chloride was added dropwise, and the reaction mixture was stirred for 5 h at 50 °C. The reaction mixture was cooled to rt and concentrated *in vacuo*. Water was added, and the aqueous solution was extracted twice with ethyl acetate. The pooled organic layers were dried over $MgSO_4$, filtered, and concentrated *in vacuo*.

*(1-Butyl-3-[(2,4-dimethoxyphenyl)methyl]-2,6-dioxo-8-{4-[(prop-2-yn-1-yl)carbamoyl]bicyclo[2.2.2]octan-1-yl}-2,3,6,7-tetrahydro-1H-purin-7-yl)methyl 2,2-Dimethylpropanoate (**22**).* **14** (600 mg, 1.10 mmol), DMF (5 mL), K_2CO_3 (227 mg, 1.64 mmol), and pivaloxymethyl chloride (214 mg, 1.42 mmol) following column elution with *n*-hexane/ethyl acetate (1:1) gave **22** (384 mg, 0.58 mmol, 52%) as a gummy liquid. ^{1}H NMR (400 MHz, DMSO-d_6): δ 0.86 (t, J = 7.4 Hz, 3H), 1.12 (s, 9H), 1.25 (m, 2H), 1.48 (m, 2H), 1.69−2.00 (m, 12H), 3.72 (s, 3H), 3.79 (s, 3H), 3.81 (t, J = 2.4 Hz, 2H), 3.85 (t, J = 7.4 Hz, 2H), 5.06 (s, 2H), 6.33 (br s, 2H), 6.42 (dd, J = 2.4, 8.4 Hz, 1H), 6.57 (d, J = 2.4 Hz, 1H), 6.80 (d, J = 8.4 Hz, 1H), 7.87 (t, J = 5.6 Hz, 1H). ^{13}C NMR (400 MHz, DMSO-d_6): δ 13.66, 19.50, 26.54, 27.45, 28.05, 29.27, 29.53, 34.55, 37.88, 38.16, 39.95, 40.92, 54.88, 55.17, 55.45, 77.29, 81.70, 98.32, 104.49, 106.65, 109.52, 116.43, 127.65, 146.79, 150.27, 153.84, 157.53, 159.78, 159.91, 176.00. HRMS (ESI) calcd for $C_{36}H_{47}NaN_5O_7^+$ $[M + Na]^+$ m/z 684.3368 and $C_{72}H_{94}NaN_{10}O_{14}^+$ $[2M + Na]^+$ m/z 1345.6843, found m/z 684.3323 and 1345.6739.

*(8-{4-[(3-Azidopropyl)carbamoyl]bicyclo[2.2.2]octan-1-yl}-1-butyl-3-[(2,4-dimethoxyphenyl)methyl]-2,6-dioxo-2,3,6,9-tetrahydro-1H-purin-9-yl)methyl 2,2-Dimethylpropanoate (**23**).* **15** (475 mg, 0.80 mmol), DMF (4 mL), K_2CO_3 (166 mg, 1.20 mmol), and pivaloxymethyl chloride (157 mg, 1.04 mmol) following column elution with *n*-hexane/ethyl acetate (1:1) gave **23** (325 mg, 0.46 mmol, 57%) as a gummy liquid. ^{1}H NMR (400 MHz, DMSO-d_6): δ 0.86 (t, J = 7.4 Hz, 3H), 1.12 (s, 9H), 1.25 (m, 2H), 1.48 (m, 2H), 1.69−2.00 (m, 12H), 3.09 (q, 2H), 3.31 (t, J = 6.8 Hz), 3.72 (s, 3H), 3.79 (s, 3H), 3.85 (t, J = 7.4 Hz, 2H), 5.06 (s, 2H), 6.33 (br s, 2H), 6.42 (dd, J = 2.4, 8.4 Hz, 1H), 6.57 (d, J = 2.4 Hz, 1H), 6.81 (d, J = 8.4 Hz, 1H), 7.46 (t, J = 5.6 Hz, 1H). ^{13}C NMR (400 MHz, DMSO-d_6): δ 13.66, 19.50, 26.54, 27.60, 28.36, 29.34, 29.53, 34.55, 36.03, 37.86, 38.16, 39.95, 40.91, 48.45, 55.17, 55.45, 69.03, 98.31, 104.49, 106.66, 116.44, 127.72, 146.79, 150.27, 153.83, 157.54, 159.79, 159.95, 175.99, 176.31. HRMS (ESI) calcd for $C_{36}H_{50}N_8NaO_7^+$ $[M + Na]^+$ m/z 729.3695, $C_{72}H_{100}N_{16}NaO_{14}^+$ $[2M + Na]^+$ m/z 1435.7497, and $C_{108}H_{150}N_{24}NaO_{21}^+$ m/z 2142.1300, found m/z 729.3659, 1435.7399, and 2143.1233.

General Procedure for DMB Deprotection and Alkylation to Give 24 and 25. The DMB-protected xanthine was dissolved in neat TFA and stirred overnight at 50 °C. The reaction mixture was cooled to rt and blown with compressed air for 20 min to evaporate excess TFA. CH_2Cl_2 was added, and the organic solution was concentrated *in vacuo* and then dried overnight under high vacuum. The residue was dissolved in DMF, K_2CO_3 added, and the reaction mixture stirred for 45 min at 50 °C. 1-Bromopropane was added dropwise, and the reaction mixture was stirred overnight at 50 °C. The reaction mixture was cooled to rt and concentrated *in vacuo*. Water was added, and the aqueous solution was extracted twice with ethyl acetate. The pooled organic layers were dried over $MgSO_4$, filtered, and concentrated *in vacuo*.

*(1-Butyl-2,6-dioxo-8-{4-[(prop-2-yn-1-yl)carbamoyl]bicyclo-[2.2.2]octan-1-yl}-3-propyl-2,3,6,7-tetrahydro-1H-purin-7-yl)methyl 2,2-Dimethylpropanoate (**24**).* **22** (370 mg, 0.56 mmol), TFA (2.5 mL), DMF (4 mL), K_2CO_3 (154 mg, 1.11 mmol), and 1-bromopropane (136 mg, 1.11 mmol) following column elution with *n*-hexane/ethyl acetate (7:3) gave **24** (239 mg, 0.43 mmol, 77%) as a gummy liquid. ^{1}H NMR (400 MHz, $CDCl_3$): δ 0.92 (t, J = 7.4 Hz, 3H), 0.97 (t, J = 7.6 Hz, 3H), 1.20 (s, 9H), 1.36 (m, 2H), 1.60 (m, 2H), 1.79 (m, 2H), 2.01−2.17 (m, 12H), 2.29 (s, 1H), 2.29 (s, 2H), 3.98 (t, J = 7.4 Hz, 2H), 4.05 (t, J = 7.2 Hz, 2H), 6.37 (br s, 2H), 6.65 (m, 1H). ^{13}C NMR (400 MHz, $CDCl_3$): δ 11.25, 11.61, 14.17, 20.55, 21.84, 27.28, 29.57, 30.13, 30.47, 33.64, 35.39, 39.14, 41.49, 45.17, 69.27, 77.56, 107.89, 122.02, 147.59, 148.86, 151.45, 154.96, 159.87, 168.63, 177.44. HRMS (ESI) calcd for $C_{30}H_{43}N_5NaO_5^+$ $[M + Na]^+$ m/z 576.3156, found m/z 576.3132.

*(8-{4-[(3-Azidopropyl)carbamoyl]bicyclo[2.2.2]octan-1-yl}-1-butyl-2,6-dioxo-3-propyl-2,3,6,9-tetrahydro-1H-purin-9-yl)methyl 2,2-Dimethylpropanoate (**25**).* **23** (288 mg, 0.41 mmol), TFA (2 mL), DMF (4 mL), K_2CO_3 (113 mg, 0.81 mmol), and 1-bromopropane (75 mg, 0.61 mmol) following column elution with *n*-hexane/ethyl acetate (8:2) gave **25** (102 mg, 0.17 mmol, 42%) as a white solid. ^{1}H NMR (400 MHz, DMSO-d_6): δ 0.86 (t, J = 7.4 Hz, 3H), 0.86 (t, J = 7.4 Hz, 3H), 1.11 (s, 9H), 1.25 (m, 2H), 1.48 (m, 2H), 1.65−2.02 (m, 16H), 3.10 (q, 2H), 3.31 (t, J = 6.8 Hz), 3.84 (t, J = 7.2 Hz, 2H), 3.93 (t, J = 6.4 Hz, 2H), 6.32 (s, 2H), 7.48 (t, J = 5.4 Hz, 1H). ^{13}C NMR (400 MHz, DMSO-d_6): δ 10.91 (d), 13.56 (d), 26.42 (d), 27.52 (d), 28.27 (d), 29.25 (d), 29.46 (d), 34.44 (d), 35.94 (d), 37.79 (d), 38.17, 43.96 (d), 48.36 (d), 56.02 (d), 68.88 (d), 106.53 (d), 109.31, 128.34 (d), 146.47 (d), 150.17 (d), 153.66 (d), 159.88 (d), 175.89 (d), 176.23 (d). HRMS (ESI) calcd for $C_{30}H_{46}N_8NaO_5^+$ $[M + Na]^+$ m/z 621.3483 and $C_{60}H_{92}N_{16}NaO_{10}^+$ $[2M + Na]^+$ m/z 1219.7075, found m/z 621.3456 and 1219.6990.

General Procedure for POM Deprotection to give UODC4 and UODC1. The POM-protected xanthine was dissolved in 2 M methanolic NaOH and stirred for 1 h. The reaction mixture was neutralized with AcOH to pH 4 and cooled overnight, and the precipitate that formed was collected by filtration, washed with water, and air-dried.

*4-(1-Butyl-2,6-dioxo-3-propyl-2,3,6,9-tetrahydro-1H-purin-8-yl)-N-(prop-2-yn-1-yl)bicyclo[2.2.2]octane-1-carboxamide (**UODC4**).* **24** (110 mg, 0.20 mmol) and NaOH (2 mL) gave **UODC4** (85 mg, 0.19 mmol, 98%) as a white fluffy solid. ^{1}H NMR (500 MHz, DMSO-

https://doi.org/10.1021/acs.jmedchem.0c02169
J. Med. Chem. 2021, 64, 8161−8178

d_6): δ 1.11 (t, J = 7.2 Hz, 3H), 1.14 (t, J = 7 Hz, 3H), 1.53 (m, 2H), 1.76 (m, 2H), 1.93 (m, 2H), 2.11−2.25 (m, 12H), 2.24 (s, 2H), 2.25 (s, 1H), 3.86 (t, J = 7.3 Hz, 2H), 3.93 (t, J = 7.3 Hz, 2H), 6.67 (s, 1H), 12.97 (s, 1H). ^{13}C NMR (500 MHz, DMSO-d_6): δ 10.52, 11.00, 13.70, 19.61, 20.86, 29.13, 29.42, 29.68, 32.93, 33.18, 39.90, 40.17, 44.22, 106.48, 122.16, 147.33, 147.78, 150.58, 153.88, 160.10, 167.75. HRMS (ESI) calcd for $C_{24}H_{33}N_5NaO_3^+$ [M + Na]$^+$ m/z 462.2476 and $C_{48}H_{66}N_{10}NaO_6^+$ [2M + Na] m/z 901.5059, found m/z 462.2436 and 901.4979. HPLC: 19.08 min.

*N-(3-Azidopropyl)-4-(1-butyl-2,6-dioxo-3-propyl-2,3,6,9-tetrahydro-1H-purin-8-yl)bicyclo[2.2.2]octane-1-carboxamide (**UODC1**).* **25** (11 mg, 0.018 mmol) and NaOH (200 μL) following column elution with n-hexane/ethyl acetate (3:7) and then semipreparative RP-HPLC purification gave **UODC1** (8 mg, 0.016 mmol, 89%) as a white solid. ^{1}H NMR (500 MHz, DMSO-d_6): δ 0.85 (t, J = 7.5 Hz, 3H), 0.89 (t, J = 7.3 Hz, 3H), 1.27 (m, 2H), 1.51 (m, 2H), 1.61−1.91 (m, 16H), 3.10 (q, J = 6.2 Hz, 2H), 3.31 (t, J = 6.8 Hz, 2H), 3.86 (t, J = 7.5 Hz, 2H), 3.92 (t, J = 7.5 Hz, 2H), 7.48 (t, J = 5.8 Hz, 1H), 12.92 (br s, 1H). ^{13}C NMR (500 MHz, DMSO-d_6): δ 11.01, 13.72, 13.94, 19.60, 20.86, 27.83, 28.39, 29.65, 29.68, 33.21, 36.06, 38.10, 39.45, 44.21, 48.47, 106.43, 147.30, 150.59, 153.88, 160.31, 176.48. HRMS (ESI) calcd for $C_{24}H_{36}N_8NaO_3^+$ [M + Na]$^+$ m/z 507.2803 and $C_{48}H_{72}N_{16}NaO_6^+$ [2M + Na]$^+$ m/z 991.5713, found m/z 507.2804 and 991.5728. HPLC: 17.76 min.

*1-Butyl-8-cyclohexyl-3-[(2,4-dimethoxyphenyl)methyl]-2,3,6,9-tetrahydro-1H-purine-2,6-dione (**26**).* According to the procedure described for **11**, cyclohexanoic acid (129 mg, 1.00 mmol), Et_3N (392 mg, 3.87 mmol), HATU (383 mg, 1.00 mmol), and **9** (351 mg, 1.00 mmol) gave **26** (391 mg, 0.88 mmol, 88%) as a white solid. ^{1}H NMR (400 MHz, DMSO-d_6): δ 0.88 (t, J = 7.2 Hz), 1.10−1.90 (m, 14H), 1.72 (m, 2H), 2.66 (m, 1H), 3.71 (s, 3H), 3.82 (s, 3H), 3.86 (t, J = 7.4 Hz), 5.04 (s, 1H), 6.39 (dd, J = 2.4, 8.4 Hz, 1H), 6.57 (d, J = 2.4 Hz), 6.66 (d, J = 8.4 Hz), 13.10 (br s, 1H). ^{13}C NMR (400 MHz, DMSO-d_6): δ 13.73, 19.63, 25.26, 25.33, 29.70, 30.95, 37.59, 40.28, 41.12, 55.19, 55.48, 98.31, 104.42, 106.05, 109.56, 116.65, 126.68, 147.79, 150.65, 153.96, 157.37, 158.25, 159.63. HRMS (ESI) calcd for $C_{24}H_{33}N_4O_4^+$ [M + H]$^+$ m/z 441.2496 and $C_{24}H_{32}N_4NaO_4^+$ [M + Na]$^+$ m/z 463.2316, found m/z 441.2496 and 463.2318.

*4-{[3-(1-Butyl-8-cyclohexyl-2,6-dioxo-2,3,6,9-tetrahydro-1H-purin-3-yl)propyl]carbamoyl}benzene-1-sulfonyl Fluoride (**UODC8**).* According to the procedure described for **UODC6**, **26** (332 mg, 0.75 mmol), TFA (2.5 mL), and 4-[(3-bromopropyl)-carbamoyl]benzenesulfonyl fluoride (370 mg, 1.14 mmol) following column chromatography eluting with n-hexane/ethyl acetate (4:6) gave **UODC8** (343 mg, 0.64 mmol, 85%) as a white solid. ^{1}H NMR (500 MHz, DMSO-d_6): δ 0.88 (t, J = 7.3 Hz, 3H), 1.12−2.00 (m, 16H), 2.62 (m, 1H), 3.31 (q, J = 6.5 Hz, 2H), 3.85 (t, J = 7.3 Hz, 2H), 4.07 (t, J = 6.8 Hz, 2H), 8.17 (d, J = 8.5 Hz, 2H), 8.26 (d, J = 8.5 Hz, 2H), 8.87 (t, J = 5.5 Hz, 1H), 13.04 (br s, 1H). ^{13}C NMR (500 MHz, DMSO-d_6): δ 13.70, 19.62, 25.18, 25.28, 25.34, 27.44, 29.68, 30.87, 36.82, 37.54, 40.20, 40.70, 106.01, 128.59, 128.99, 192.23 (d), 141.62, 147.51, 150.60, 150.93, 153.86, 158.13, 164.24. ^{19}F NMR (400 MHz, DMSO-d_6): δ 66.04. HRMS (ESI) calcd for $C_{25}H_{31}FN_5O_5S^-$ [M − H]$^-$ m/z 532.2035, found m/z 532.2068. HPLC: 19.52 min.

Molecular Modeling and Docking. The three-dimensional structure of **UODC2** was generated using Avogadro 1.2.0[33] and minimized using the universal force field (UFF). Ligand docking was performed using GOLD 5.8.1 (CCDC Software)[34] centered on residues F171 (A_1R) and F168 (A_3R homology model) with a distance extension of 15 Å. The covalent binding mode was used, and the covalent link was defined between position 4 of Y271$^{7.36}$ (A_1R) or Y265$^{7.36}$ (A_3R homology model) and the oxygen atom of the sulfonyl moiety (SO_3). The highest-ranked pose at each receptor is presented. The docking results were visualized in PyMOL (The PyMOL Molecular Graphics System, version 2.3.2, Schrödinger, LLC). The A_3R homology model was generated using Modeler 9.22[35] based on the antagonist-bound DU172-A_1R crystal structure (PDB entry 5UEN),[22] which includes the command "a.md_level = refine.slow" that performs a thorough MD optimization. All structures were protonated appropriately prior to docking via either PyMOL or Hermes. Hydrogen atoms were added to both the A_1R crystal structure and the A_3R homology model prior to docking. DU172 was successfully docked into the ligand-free receptor from the A_1R crystal structure (PDB entry 5UEN) using covalent docking protocols as a positive control.

Biology. All novel compounds, including all novel assayed compounds, were screened for PAINS using https://www.cbligand.org/PAINS/search_struct.php, and all compounds passed the filter. Dulbecco's modified Eagle's medium (DMEM), fetal bovine serum (FBS), trypsin, and the Pierce BCA protein assay kit were purchased from Invitrogen (Carlsbad, CA). Adenosine deaminase (ADA) and hygromycin B were purchased from Roche Diagnostics (Mannheim, Germany). Ultima Gold scintillation cocktail, MicroScint-O, [^{3}H]DPCPX {8-cyclopentyl-1,3-dipropylxanthine, [dipropyl-2,3-3H-(N)]}, and the LANCE cAMP kit were purchased from PerkinElmer Life Sciences (Glen Waverley, Australia). Adenosine receptor ligands, 8-{4-[4-(4-chlorophenyl)piperazide-1-sulfonyl]phenyl}-1-propylxanthine (PSB-603), N-[9-chloro-2-(2-furanyl)[1,2,4]-triazolo[1,5-c]-quinazolin-5-yl]benzene acetamide (MRS1220), 2-(2-furanyl)-7-[3-(4-methoxyphenyl)propyl]-7H-pyrazolo[4,3-e][1,2,4]triazolo[1,5-c]-pyrimidin-5-amine (SCH442416), and *trans*-4-[(2-phenyl-7H-pyrrolo-[2,3-d]pyrimidin-4-yl)amino]cyclohexanol (SLV320) were purchased from Tocris Bioscience (Bristol, U.K.). CA200645, the fluorescent A_3 antagonist, was from Hello Bio (Bristol, U.K.), while furimazine was from Promega (Alexandria, Australia). Unless stated otherwise, all other reagents ordered from Sigma-Aldrich (Castle Hill, Australia) were of analytical quality.

Cell Culture and Membrane Preparation. Nontransfected HEK293 adherent (NT-HEK293A) and nontransfected FlpIn Chinese hamster ovary (NT-FlpInCHO) cells were maintained in DMEM supplemented with 5% FBS and 16 mM HEPES. FlpInCHO cells stably transfected with the human A_1, A_{2A}, A_{2B}, or A_3 adenosine receptor (A_1R-FlpInCHO, A_{2A}R-FlpInCHO, A_{2B}R-FlpInCHO, or A_3R-FlpInCHO, respectively) were grown in DMEM supplemented with 5% FBS, 16 mM HEPES, and hygromycin B (500 μg/mL). All cells were maintained at 37 °C in a 5% CO_2 humidified incubator, grown to confluence, and then seeded in 96-well culture plates at assay-specific densities. Membrane preparation was performed as previously described.[36] The protein content was determined using a Pierce BCA protein assay kit according to the manufacturer's instructions.

cAMP Accumulation. The A_1R-, A_{2A}R-, A_{2B}R-, and A_3R-FlpInCHO cells were seeded into 96-well culture plates at a density of 30000 cells/well and incubated overnight at 37 °C in a 5% CO_2 incubator. The cAMP assays were performed as described previously.[37] Ligand concentration−response curves were normalized to the baseline response (0%) mediated by 3 μM forskolin (A_1R- and A_3R-FlpInCHO) or buffer (A_{2A}R- and A_{2B}R-FlpInCHO) and the maximal response (100%) mediated by buffer (A_1R- and A_3R-FlpInCHO) or 3 μM forskolin (A_{2A}R- and A_{2B}R-FlpInCHO).

[^{3}H]DPCPX Binding Assay Using A_1R-FlpInCHO Membranes and Whole Cells. Radioligand binding experiments were performed in binding buffer [10 mM HEPES, 10 mM D-glucose, 145 mM NaCl, 5 mM KCl, 1 mM $MgSO_4$, 1.5 mM $NaHCO_3$, 2 mM $CaCl_2$, and 1 unit/mL ADA (pH 7.4)]. Membrane homogenates of A_1AR-FlpInCHO (15 μg) were incubated with different concentrations of competing ligands in the presence of approximately 1 nM [^{3}H]DPCPX (precise concentrations in each experiment were determined by β-counting) for 4 h at 25 °C. Incubation was terminated by rapid filtration through UniFilter-96 GF/C (Whatman) microplates using a Filtermate 96 harvester (Packard). Filter plates were washed three times with ice-cold 0.9% NaCl, dried overnight before the addition of MicroScint-O scintillation cocktail (40 μL/well), and allowed to stand for at least 1 h before radioactivity was determined by β-counting using a MicroBeta 2 LumiJET microplate counter (PerkinElmer).

To assess the irreversible binding of selected clickable probes, A_1R-FlpInCHO cells were plated in 96-well poly-D-lysine isoplates at a density of 40000 cells/well and incubated overnight at 37 °C in a 5% CO_2 incubator. After removal of cell media, cells were incubated with increasing concentrations of competing ligands for 3 h in binding buffer, followed by extensive washing steps (6 × 20 min, total of 2 h) at room temperature. Cells were incubated with approximately 1 nM

https://doi.org/10.1021/acs.jmedchem.0c02169
J. Med. Chem. 2021, 64, 8161−8178

[^{3}H]DPCPX (precise concentrations in each experiment were determined by β-counting) for 4 h at 4 °C. Upon removal of the radioligand, cells were washed five times with ice-cold phosphate-buffered saline (PBS) (10 mM Na_2HPO_4, 1.8 mM KH_2PO_4, 137 mM NaCl, and 2.7 mM KCl) and dissolved in Ultima Gold scintillation liquid (100 μL/well). Isoplates were sealed and allowed to incubate for at least 1 h before radioactivity was determined by β-counting using a MicroBeta 2 LumiJET microplate counter (PerkinElmer). For all radioligand binding experiments, nonspecific binding was assessed using 1 μM SLV320, a selective A_1R antagonist. After subtraction of the nonspecific binding, competition binding data were normalized to radioligand binding values in the absence of competitors and fitted to the one-site competition binding equation in Prism 8.0 (GraphPad) to derive log K_i values.

NanoBRET Binding Displacement Assay. Nontransfected HEK293A cells were transiently transfected with 3 μg of cDNA of N-terminal NanoLuc (Nluc)-tagged A_3R using polyethylenimine (PEI) at a 4:1 ratio in 10 cm dishes. Twenty-four hours post-transfection, cells were seeded into 96-well poly-D-lysine solid white bottom plates at a density of 40000 cells/well and incubated overnight at 37 °C in a 5% CO_2 incubator in serum-free DMEM. On the day of the assay, 48 h post-transfection, cells were incubated with increasing concentrations of competing ligands for 3 h, prepared in a binding buffer. After ligand incubation, 5 nM CA200645 was added for 60 min at room temperature and then the NLuc substrate furimazine was added to a final concentration of 10 μM. Sequential emission measurements were taken using a PHERAStar Omega plate reader (BMG Labtech) using 460 nm (80 nm bandpass, donor NLuc emission) and 610 nm (long-pass filter, fluorescent ligand emission) filters at 25 °C. Raw BRET ratios were calculated by dividing the 610 nm emission (acceptor) by the 460 nm emission (donor). To assess irreversible binding of selected clickable probes, 6 × 20 min (total of 2 h) extensive washing steps were added before the addition of a fluorescent antagonist and furimazine. In all NanoBRET binding experiments, nonspecific binding was assessed using 1 μM MRS1220, a selective A_3R antagonist. After subtraction of the nonspecific binding, competition binding data were normalized to total binding values in the presence of a vehicle and fitted to the one-site competition binding equation in Prism 8.0 (GraphPad) yielding log K_i values.

Whole Cell Affinity Labeling and SDS−PAGE. Nontransfected FlpInCHO cells and A_1R-FlpInCHO cells were incubated with clickable probes at indicated concentrations (0.1, 1, and 10 μM) or a vehicle control (0.1% DMSO) in a binding buffer for 90 min. Cells were washed twice with PBS (10 min/wash, gentle shaking), lifted from the plate, and centrifuged (300*g* for 5 min at rt). Then, cell pellets were resuspended in a click chemistry conjugation reaction mixture for 1 h at rt with intermittent vortexing. The click reagents were added in the following sequence: 1 μM fluorescent Cy5.5 azide or Cy5.5 alkyne (Lumiprobe), 1 mM ascorbic acid (made immediately prior to use), TBTA/*tert*-butanol, and 1 mM $CuSO_4$. Following click chemistry, unbound click reagents were washed off by centrifugation of the samples (300*g* for 5 min at rt) and resuspending the material in PBS once before resuspending the cells in a radioimmunoprecipitation assay (RIPA) lysis buffer (10 mM Tris, 2 mM EDTA, 20 mM β-glycerophosphate, 0.1% NP40, 100 mM NaCl, and 12 mM sodium deoxycholate) for 10 min at 4 °C. Cell lysates were then centrifuged (16000*g* for 10 min at 4 °C), and the protein concentration of the supernatant was determined by the Pierce BCA protein assay. After normalization of the protein concentration, 4× SDS loading buffer was added and the protein material denatured for 30 min at 37 °C. Proteins were separated by SDS−PAGE on 10% polyacrylamide gels (200 V for 50 min at rt). In-gel fluorescence was detected using a Typhoon system (Amersham). Proteins were subsequently transferred to nitrocellulose membranes (20 V overnight at 4 °C), and membranes were blocked with Odyssey blocking buffer and incubated with the anti-V5 (1:2500, mouse monoclonal, Sigma) or anti-β-actin (1:2500, rabbit polyclonal, Abcam) antibody overnight at 4 °C. Thereafter, membranes were washed three times (20 min/wash) with PBS-T (PBS with 0.1% Tween 20) and incubated with the donkey anti-mouse 488 (1:10000, Abcam) or donkey anti-rabbit 488 (1:10000, Abcam) antibody for 2h at rt. Following three washes with PBST, membranes were imaged using the Typhoon system (Amersham). The signal intensities of the Cy5.5 click tag and secondary antibodies were quantified using ImageStudio (LiCOR). The Cy5.5 fluorescence was normalized to the relative V5 level (for A_1R-FlpInCHO cells) or β-actin level (for nontransfected FlpIn CHO cells) in each sample. To assess nonspecific protein labeling, prior to the two-step labeling experiment, A_1R-FlpInCHO cells were preincubated with 10 μM UODC6 or a vehicle control (0.1% DMSO) for 90 min, followed by labeling with either 1 or 10 μM clickable probes for an additional 90 min. Samples were then subjected to the click chemistry procedure using the protocol described above.

Data Analysis. Nonlinear regression curve fitting and statistical analyses were performed using Prism 8.0 (GraphPad Software Inc., San Diego, CA). To derive potency estimates, agonist concentration−response data were fitted to a three-parameter Hill equation as described previously.[10] Radioligand inhibition binding data with competitive ligands were fitted to a one-site inhibition mass action curve. Resulting IC_{50} values were converted to dissociation constants (K_i values) using the Cheng−Prusoff equation.[38] To estimate antagonist affinity values, functional interaction studies between NECA and multiple concentrations of each antagonist in the cAMP assays were fitted to the competitive model as described previously.[22] All results were expressed as means ± SEM.

■ ASSOCIATED CONTENT

Supporting Information

The Supporting Information is available free of charge at https://pubs.acs.org/doi/10.1021/acs.jmedchem.0c02169.

Molecular formula strings of the prepared compounds (CSV)

A_3AR homology model (PDB)

Additional synthetic details such as the concentration−response curves for data reported in Tables 1 and 2 (Figures S1−S3), docking of UODC2 into the A_{2A}R (PDB entry 6LPK) (Figure S4), and an immunoblotting control experiment (Figure S5) (PDF)

■ AUTHOR INFORMATION

Corresponding Authors

Lauren T. May − *Drug Discovery Biology, Monash Institute of Pharmaceutical Sciences, and Department of Pharmacology, Monash University, Parkville, VIC 3052, Australia*; Email: lauren.may@monash.edu

Andrea J. Vernall − *Department of Chemistry, University of Otago, Dunedin 9016, New Zealand*; orcid.org/0000-0001-8056-0726; Email: andrea.vernall@otago.ac.nz

Karen J. Gregory − *Drug Discovery Biology, Monash Institute of Pharmaceutical Sciences, and Department of Pharmacology, Monash University, Parkville, VIC 3052, Australia*; orcid.org/0000-0002-3833-2137; Email: karen.gregory@monash.edu

Authors

Phuc N. H. Trinh − *Drug Discovery Biology, Monash Institute of Pharmaceutical Sciences, and Department of Pharmacology, Monash University, Parkville, VIC 3052, Australia*

Daniel J. W. Chong − *School of Pharmacy, University of Otago, Dunedin 9016, New Zealand*

Katie Leach − *Drug Discovery Biology, Monash Institute of Pharmaceutical Sciences, and Department of Pharmacology, Monash University, Parkville, VIC 3052, Australia*; orcid.org/0000-0002-9280-1803

Stephen J. Hill − *Centre of Membrane Proteins and Receptors (COMPARE), University of Birmingham and University of Nottingham, The Midlands NG7 2UH, U.K.; Division of*

Physiology, Pharmacology and Neuroscience, School of Life Sciences, University of Nottingham, Nottingham NG7 2UH, U.K.; orcid.org/0000-0002-4424-239X

Joel D. A. Tyndall − *School of Pharmacy, University of Otago, Dunedin 9016, New Zealand;* orcid.org/0000-0003-0783-1635

Complete contact information is available at: https://pubs.acs.org/10.1021/acs.jmedchem.0c02169

Author Contributions

P.N.H.T. and D.J.W.C. contributed equally to this work. K.L., J.D.A.T., L.T.M., A.J.V., and K.J.G. participated in study design. D.J.W.C., J.D.A.T., and A.J.V. conducted and/or analyzed medicinal chemistry and computational experiments. P.N.H.T. and K.J.G. performed pharmacology and biochemical experiments. P.N.H.T., L.T.M., and K.J.G. performed data analysis and interpretations of pharmacological experiments. S.J.H. contributed tools or reagents. P.N.H.T., D.J.W.C., A.J.V., L.T.M., and K.J.G. wrote the manuscript. All authors edited and approved the final manuscript.

Notes

The authors declare no competing financial interest.

■ ACKNOWLEDGMENTS

This work was supported by National Health and Medical Research Council of Australia (NHMRC) Project Grants APP1123722 (K.J.G., L.T.M., and A.J.V.), APP1145420 (L.T.M. and S.J.H.), and APP1147291 (L.T.M.). L.T.M. is an Australian National Heart Foundation Future Leaders Fellow. K.J.G. and K.L are supported by Australian Research Council Future Fellowships (FT160100075 and FT170100392). D.J.W.C. was supported by a University of Otago Doctoral Scholarship.

■ ABBREVIATIONS USED

A_1R, adenosine A_1 receptor; $A_{2A}R$, adenosine $A_{2A}R$ receptor; $A_{2B}R$, adenosine $A_{2B}R$ receptor; A_3R, adenosine A_3 receptor; ACN, acetonitrile; AcOH, acetic acid; AR, adenosine receptor; br, broad; CCDC, Cambridge Crystallographic Data Centre; CHO, Chinese hamster ovary; COSY, homonuclear correlation spectroscopy; DIPEA, diisopropylethylamine; DMB, 3,4-dimethoxybenzyl; DMF, dimethylformamide; DMSO, dimethyl sulfoxide; GPCR, G protein-coupled receptor; HATU, *O*-(7-azabenzotriazol-1-yl)-*N*,*N*,*N*′,*N*′-tetramethyluronium hexafluorophosphate; HEK, human embryonic kidney; HMBC, heteronuclear multiple-bond correlation; HPLC, high-performance liquid chromatography; HRMS, high-resolution mass spectrometry; HSQC, heteronuclear single-quantum coherence; NMR, nuclear magnetic resonance; NOESY, nuclear Overhauser effect spectroscopy; PDB, Protein Data Bank; PEG, polyethylene glycol; POM, pivaloyloxymethyl; POM-Cl, chloromethyl pivalate; RP-HPLC, reverse-phase HPLC; SAR, structure−activity relationship; SDS−PAGE, sodium dodecyl sulfate−polyacrylamide gel electrophoresis; SEM, standard error of the mean; TBAB, tetra-*n*-butylammonium bromide; TFA, trifluoroacetic acid; TLC, thin layer chromatography; TR-FRET, time-resolved fluorescence resonance energy transfer; UFF, universal force field

■ REFERENCES

(1) Chen, J. F.; Eltzschig, H. K.; Fredholm, B. B. Adenosine Receptors as Drug Targets–What Are the Challenges? *Nat. Rev. Drug Discovery* **2013**, *12*, 265−286.

(2) Fredholm, B. B.; Arslan, G.; Halldner, L.; Kull, B.; Schulte, G.; Wasserman, W. Structure and Function of Adenosine Receptors and Their Genes. *Naunyn-Schmiedeberg's Arch. Pharmacol.* **2000**, *362*, 364−374.

(3) Shryock, J. C.; Belardinelli, L. Adenosine and Adenosine Receptors in the Cardiovascular System: Biochemistry, Physiology, and Pharmacology. *Am. J. Cardiol.* **1997**, *79*, 2−10.

(4) Headrick, J. P.; Ashton, K. J.; Rose'meyer, R. B.; Peart, J. N. Cardiovascular Adenosine Receptors: Expression, Actions and Interactions. *Pharmacol. Ther.* **2013**, *140*, 92−111.

(5) Jacobson, K. A.; Gao, Z. G. Adenosine Receptors as Therapeutic Targets. *Nat. Rev. Drug Discovery* **2006**, *5*, 247−264.

(6) Muller, C. E.; Jacobson, K. A. Recent Developments in Adenosine Receptor Ligands and Their Potential as Novel Drugs. *Biochim. Biophys. Acta, Biomembr.* **2011**, *1808*, 1290−1308.

(7) Voors, A. A.; Dittrich, H. C.; Massie, B. M.; DeLucca, P.; Mansoor, G. A.; Metra, M.; Cotter, G.; Weatherley, B. D.; Ponikowski, P.; Teerlink, J. R.; Cleland, J. G.; O'Connor, C. M.; Givertz, M. M. Effects of the Adenosine A1 Receptor Antagonist Rolofylline on Renal Function in Patients with Acute Heart Failure and Renal Dysfunction: Results from Protect (Placebo-Controlled Randomized Study of the Selective Adenosine A1 Receptor Antagonist Rolofylline for Patients Hospitalized with Acute Decompensated Heart Failure and Volume Overload to Assess Treatment Effect on Congestion and Renal Function). *J. Am. Coll. Cardiol.* **2011**, *57*, 1899−1907.

(8) Yang, Z.; Cerniway, R. J.; Byford, A. M.; Berr, S. S.; French, B. A.; Matherne, G. P. Cardiac Overexpression of A1-Adenosine Receptor Protects Intact Mice against Myocardial Infarction. *Am. J. Phys. Heart Circ. Physiol.* **2002**, *282*, H949−955.

(9) Vecchio, E. A.; Baltos, J. A.; Nguyen, A. T. N.; Christopoulos, A.; White, P. J.; May, L. T. New Paradigms in Adenosine Receptor Pharmacology: Allostery, Oligomerization and Biased Agonism. *Br. J. Pharmacol.* **2018**, *175*, 4036−4046.

(10) Baltos, J. A.; Gregory, K. J.; White, P. J.; Sexton, P. M.; Christopoulos, A.; May, L. T. Quantification of Adenosine a(1) Receptor Biased Agonism: Implications for Drug Discovery. *Biochem. Pharmacol.* **2016**, *99*, 101−112.

(11) Valant, C.; May, L. T.; Aurelio, L.; Chuo, C. H.; White, P. J.; Baltos, J.-A.; Sexton, P. M.; Scammells, P. J.; Christopoulos, A. Separation of on-Target Efficacy from Adverse Effects through Rational Design of a Bitopic Adenosine Receptor Agonist. *Proc. Natl. Acad. Sci. U. S. A.* **2014**, *111*, 4614.

(12) Briddon, S. J.; Middleton, R. J.; Cordeaux, Y.; Flavin, F. M.; Weinstein, J. A.; George, M. W.; Kellam, B.; Hill, S. J. Quantitative Analysis of the Formation and Diffusion of A1-Adenosine Receptor-Antagonist Complexes in Single Living Cells. *Proc. Natl. Acad. Sci. U. S. A.* **2004**, *101*, 4673−4678.

(13) Ciruela, F.; Fernández-Dueñas, V.; Jacobson, K. A. Lighting up G Protein-Coupled Purinergic Receptors with Engineered Fluorescent Ligands. *Neuropharmacology* **2015**, *98*, 58−67.

(14) Stoddart, L. A.; Vernall, A. J.; Denman, J. L.; Briddon, S. J.; Kellam, B.; Hill, S. J. Fragment Screening at Adenosine-a(3) Receptors in Living Cells Using a Fluorescence-Based Binding Assay. *Chem. Biol.* **2012**, *19*, 1105−1115.

(15) Baker, J. G.; Middleton, R.; Adams, L.; May, L. T.; Briddon, S. J.; Kellam, B.; Hill, S. J. Influence of Fluorophore and Linker Composition on the Pharmacology of Fluorescent Adenosine A1 Receptor Ligands. *Br. J. Pharmacol.* **2010**, *159*, 772−786.

(16) Sexton, M.; Woodruff, G.; Horne, E. A.; Lin, Y. H.; Muccioli, G. G.; Bai, M.; Stern, E.; Bornhop, D. J.; Stella, N. Nir-Mbc94, a Fluorescent Ligand That Binds to Endogenous Cb(2) Receptors and Is Amenable to High-Throughput Screening. *Chem. Biol.* **2011**, *18*, 563−568.

(17) Vernall, A. J.; Stoddart, L. A.; Briddon, S. J.; Ng, H. W.; Laughton, C. A.; Doughty, S. W.; Hill, S. J.; Kellam, B. Conversion of a Non-

Selective Adenosine Receptor Antagonist into A3-Selective High Affinity Fluorescent Probes Using Peptide-Based Linkers. *Org. Biomol. Chem.* **2013**, *11*, 5673−5682.
(18) Hellyer, S. D.; Aggarwal, S.; Chen, A. N. Y.; Leach, K.; Lapinsky, D. J.; Gregory, K. J. Development of Clickable Photoaffinity Ligands for Metabotropic Glutamate Receptor 2 Based on Two Positive Allosteric Modulator Chemotypes. *ACS Chem. Neurosci.* **2020**, *11*, 1597−1609.
(19) Gregory, K. J.; Velagaleti, R.; Thal, D. M.; Brady, R. M.; Christopoulos, A.; Conn, P. J.; Lapinsky, D. J. Clickable Photoaffinity Ligands for Metabotropic Glutamate Receptor 5 Based on Select Acetylenic Negative Allosteric Modulators. *ACS Chem. Biol.* **2016**, *11*, 1870−1879.
(20) Soethoudt, M.; Stolze, S. C.; Westphal, M. V.; van Stralen, L.; Martella, A.; van Rooden, E. J.; Guba, W.; Varga, Z. V.; Deng, H.; van Kasteren, S. I.; Grether, U.; IJzerman, A. P.; Pacher, P.; Carreira, E. M.; Overkleeft, H. S.; Ioan-Facsinay, A.; Heitman, L. H.; van der Stelt, M. Selective Photoaffinity Probe That Enables Assessment of Cannabinoid Cb2 Receptor Expression and Ligand Engagement in Human Cells. *J. Am. Chem. Soc.* **2018**, *140*, 6067−6075.
(21) Yang, X.; Michiels, T. J. M.; de Jong, C.; Soethoudt, M.; Dekker, N.; Gordon, E.; van der Stelt, M.; Heitman, L. H.; van der Es, D.; IJzerman, A. P. An Affinity-Based Probe for the Human Adenosine A2a Receptor. *J. Med. Chem.* **2018**, *61*, 7892−7901.
(22) Glukhova, A.; Thal, D. M.; Nguyen, A. T.; Vecchio, E. A.; Jorg, M.; Scammells, P. J.; May, L. T.; Sexton, P. M.; Christopoulos, A. Structure of the Adenosine A1 Receptor Reveals the Basis for Subtype Selectivity. *Cell* **2017**, *168*, 867−877.e13.
(23) Cheng, R. K. Y.; Segala, E.; Robertson, N.; Deflorian, F.; Dore, A. S.; Errey, J. C.; Fiez-Vandal, C.; Marshall, F. H.; Cooke, R. M. Structures of Human A1 and A2a Adenosine Receptors with Xanthines Reveal Determinants of Selectivity. *Structure* **2017**, *25*, 1275−1285.e4.
(24) Kiesman, W. F.; Zhao, J.; Conlon, P. R.; Dowling, J. E.; Petter, R. C.; Lutterodt, F.; Jin, X.; Smits, G.; Fure, M.; Jayaraj, A.; Kim, J.; Sullivan, G.; Linden, J. Potent and Orally Bioavailable 8-Bicyclo[2.2.2]-Octylxanthines as Adenosine A1 Receptor Antagonists. *J. Med. Chem.* **2006**, *49*, 7119−7131.
(25) Holschbach, M. H.; Bier, D.; Wutz, W.; Willbold, S.; Olsson, R. A. Synthesis of the Main Metabolite in Human Blood of the A1 Adenosine Receptor Ligand [18f]Cpfpx. *Org. Lett.* **2009**, *11*, 4266−4269.
(26) May, L. T.; Avlani, V. A.; Langmead, C. J.; Herdon, H. J.; Wood, M. D.; Sexton, P. M.; Christopoulos, A. Structure-Function Studies of Allosteric Agonism at M2Muscarinic Acetylcholine Receptors. *Mol. Pharmacol.* **2007**, *72*, 463−476.
(27) Beauglehole, A. R.; Baker, S. P.; Scammells, P. J. Fluorosulfonyl-Substituted Xanthines as Selective Irreversible Antagonists for the a(1)-Adenosine Receptor. *J. Med. Chem.* **2000**, *43*, 4973−4980.
(28) Yang, X.; van Veldhoven, J. P. D.; Offringa, J.; Kuiper, B. J.; Lenselink, E. B.; Heitman, L. H.; van der Es, D.; IJzerman, A. P. Development of Covalent Ligands for G Protein-Coupled Receptors: A Case for the Human Adenosine a(3) Receptor. *J. Med. Chem.* **2019**, *62*, 3539−3552.
(29) Lebon, G.; Edwards, P. C.; Leslie, A. G.; Tate, C. G. Molecular Determinants of Cgs21680 Binding to the Human Adenosine A2a Receptor. *Mol. Pharmacol.* **2015**, *87*, 907−915.
(30) Pubchem Gene Summary for Ncbi Gene 136, Adora2b - Adenosine A2b Receptor (Human). 2020.
(31) Ihara, K.; Hato, M.; Nakane, T.; Yamashita, K.; Kimura-Someya, T.; Hosaka, T.; Ishizuka-Katsura, Y.; Tanaka, R.; Tanaka, T.; Sugahara, M.; Hirata, K.; Yamamoto, M.; Nureki, O.; Tono, K.; Nango, E.; Iwata, S.; Shirouzu, M. Isoprenoid-Chained Lipid Erococ17 + 4: A New Matrix for Membrane Protein Crystallization and a Crystal Delivery Medium in Serial Femtosecond Crystallography. *Sci. Rep.* **2020**, *10*, 19305.
(32) Uhlen, M.; Fagerberg, L.; Hallstrom, B. M.; Lindskog, C.; Oksvold, P.; Mardinoglu, A.; Sivertsson, A.; Kampf, C.; Sjostedt, E.; Asplund, A.; Olsson, I.; Edlund, K.; Lundberg, E.; Navani, S.; Szigyarto, C. A.; Odeberg, J.; Djureinovic, D.; Takanen, J. O.; Hober, S.; Alm, T.; Edqvist, P. H.; Berling, H.; Tegel, H.; Mulder, J.; Rockberg, J.; Nilsson, P.; Schwenk, J. M.; Hamsten, M.; von Feilitzen, K.; Forsberg, M.; Persson, L.; Johansson, F.; Zwahlen, M.; von Heijne, G.; Nielsen, J.; Ponten, F. Proteomics. Tissue-Based Map of the Human Proteome. *Science* **2015**, *347*, 1260419.
(33) Hanwell, M. D.; Curtis, D. E.; Lonie, D. C.; Vandermeersch, T.; Zurek, E.; Hutchison, G. R. Avogadro: An Advanced Semantic Chemical Editor, Visualization, and Analysis Platform. *J. Cheminf.* **2012**, *4*, 17.
(34) Jones, G.; Willett, P.; Glen, R. C.; Leach, A. R.; Taylor, R. Development and Validation of a Genetic Algorithm for Flexible Docking. *J. Mol. Biol.* **1997**, *267*, 727−748.
(35) Sali, A.; Blundell, T. L. Comparative Protein Modelling by Satisfaction of Spatial Restraints. *J. Mol. Biol.* **1993**, *234*, 779−815.
(36) May, L. T.; Sexton, P. M.; Christopoulos, A. Effects of Urea Pretreatment on the Binding Properties of Adenosine A1 Receptors. *Br. J. Pharmacol.* **2005**, *146*, 1119−1129.
(37) Aurelio, L.; Baltos, J. A.; Ford, L.; Nguyen, A. T. N.; Jörg, M.; Devine, S. M.; Valant, C.; White, P. J.; Christopoulos, A.; May, L. T.; Scammells, P. J. A Structure-Activity Relationship Study of Bitopic N(6)-Substituted Adenosine Derivatives as Biased Adenosine a(1) Receptor Agonists. *J. Med. Chem.* **2018**, *61*, 2087−2103.
(38) Cheng, Y.; Prusoff, W. H. Relationship between the Inhibition Constant (K1) and the Concentration of Inhibitor Which Causes 50 Per Cent Inhibition (I50) of an Enzymatic Reaction. *Biochem. Pharmacol.* **1973**, *22*, 3099−3108.

https://doi.org/10.1021/acs.jmedchem.0c02169
J. Med. Chem. 2021, 64, 8161−8178